LAPPEENRANTA UNIVERSITY OF TECHNOLOGY
Faculty of Technology
Degree Program in Energy Technology

Author of the thesis Sumin Mikhail

HEAT FLUX MEASUREMENT INSIDE INTERNAL COMBUSTION ENGINE WITH GRADIENT HEAT FLUX SENSOR

Examiners: D.Sc. Andrey Mityakov
D.Sc. Esa Vakkilainen

ABSTRACT

Lappeenranta University of Technology
Faculty of Technology
Degree Programme in Energy Technology

Mikhail Sumin

Heat flux measurement inside internal combustion engine with gradient heat flux sensor.

Master's thesis
2013
79 pages, 28 figures, 3 tables

Examiners: Andrey Mityakov, Esa Vakkilainen

Keywords: Heat flux sensors, internal combustion engine, heat transfer modeling.

This master's thesis is devoted to study different heat flux measurement techniques such as differential temperature sensors, semi-infinite surface temperature methods, calorimetric sensors and gradient heat flux sensors. The possibility to use Gradient Heat Flux Sensors (GHFS) to measure heat flux in the combustion chamber of compression ignited reciprocating internal combustion engines was considered in more detail. A. Mityakov conducted an experiment, where Gradient Heat Flux Sensor was placed in four stroke diesel engine Indenor XL4D to measure heat flux in the combustion chamber. The results which were obtained from the experiment were compared with model's numerical output. This model (a one – dimensional single zone model) was implemented with help of MathCAD and the result of this implementation is graph of heat flux in combustion chamber in relation to the crank angle. The values of heat flux throughout the cycle obtained with aid of heat flux sensor and theoretically were sufficiently similar, but not identical. Such deviation is rather common for this type of experiment.

TABLE OF CONTENTS

LIST OF SYMBOLS AND ABBREVIATIONS

a - Wiebe function parameters;

a_{th} - thermal diffusivity of the material (m^2/s);

A - cross section area of the probe (m^2);

A_{ac} - the active surface area (m^2);

A_{an} – anisotropic thermoelement's area (m^2);

A_n - the amplitude functions;

A_v - the reference valve area (m^2);

b - the cylinder bore (m);

B_n - the amplitude functions;

c_v - the specific heat at constant volume (J/(kg*K));

C_D - the valve discharge coefficient;

C_p – specific heat capacity (J/(kg*K));

C_{p_a} - thermal capacity of gases (mole / h);

$C_{p_{tur}}$ - thermal capacity of air (mole / h);

C_{pc} - specific heat of water (J/(kg*K));;

e – thermo – EMF (V);

E - voltage output (V/m);

E_T - electric field vector (V/m);

h - enthalpy (J/kg);

h_T - heat transfer coefficient (W/(m^2*K));

I_o - the amount of air (kg);

k - the thermal conductivity (W/(m*K));

k_{xx}, k_{zz} - components of the thermal conductivity tensors.

K_k - dimensionless value for thermal conductivity;

K_δ - layers thickness ratio.

K_σ - dimensionless value for electric conductivity;

l_c - length of the connecting rod (m);

l × w × h – sensor dimensions (m);

L - amount of the air (mole/kg);

Le - the effective work (J);

Li - indicated complete work (J);

L_M - the mechanical work (J);

L_o - the amount of air (mole);

m - gas mass in the cylinder;

m_{fuel} - cylinder mass content (kg);

m_{sys} - mass of the system (kg);

$\dot{m}_c$ - water mass flow rate (kg);

M_a - hour consumption of air (mole / h);

M_g - hour consumption of the fulfilled gases (mole / h);

M_r - amount of the residual gases (mole/kg);

N - a number of thermocouple junction pairs;

N - number of members of the row;

n - the current number of members of the row;

n_1 - indicator polytrope;

n_2 - mean value of the expansion polytrope indicator;

n_k - a polytropic index of air compression;

n_w - Wiebe function parameters;

p_a - pressure of a charge at the end of filling;

p_b - pressure at the end of the expansion (Pa);

p_k - pressurization pressure (Pa);

p_r - residual gases pressure (Pa);

p_z - maximum combustion pressure (Pa);

Δp_x - air cooler resistibility (Pa);

q - heat flux density on a surface (W/m^2);

q_z - heat flux per unit area (W/m^2);

$\vec{q}$ - heat flux (W/m^2);

$\dot{q}$ - heat flux rate (W/m^2);

q'' - the one-dimensional heat flux (W/m^2);

Q - net heat into the cylinder (J);

Q_c - heat release during the combustion process (J);

Q_{com} - heat loss in compression process (J);

Q_{cool} - losses with the cooling environment (J);

$Q_{c\text{-}e}$ - heat loss in combustion and expansion process (J);

Q_{dis} – dissociation;

Q_e - useful heat (J);

Q_{fil} - filling heat (J);

Q_{ful} - the fulfilled gases (J);

Q_{ht} - heat transfer through the cylinder walls (J);

Q_{ic} - combustion incompleteness;

Q_{imb} – imbalance (J);

$Q_{p\text{-}c}$ - heat loss on friction (J);

Q_{rel} - release heat (J);

Q_t - total chemical energy (J);

Q_{tur} - turbine heat loss (J);

Q_{wp} - water pumps heat loss;

Q_{LHV} - lower heating value (J/kg);

Q_{ω} - losses in cooled water;

r - compression ratio;

R - an active radius of the foil (m);

R - gas constant (J/(mole*K));

s - the thickness of the foil (m);

s_c - stroke (m);

S - thermoelectric sensitivity (V/W);

S_0 - sensitivity (V/W);

S_T - the Seebeck coefficient (V/K);

t_k - booster air temperature (K);

T - the mean cylinder gas temperature (K);

T_a - charge temperature in the cylinder at the end of filling (K);

T_b - temperature at the end of the expansion (K);

T_i - the initial temperature (K);

T_k - air temperature in a booster receiver (K);

T_k - air temperature in front of the inlet valve (K);

T_m - average temperatures on depth δ of the piston (K);

T_r - temperature of the fluid (K);

T_r - residual gases temperature (K);

T_s - surface temperature (K);

T_{tur} - air temperature behind the turbine (K);

T_w - average temperature of walls (K);

T_w - the cylinder wall temperature (K);

T_z - combustion temperature (K);

T_0 - gases temperature behind the turbine (K);

T_l - average temperatures on the bottom of the piston (K);

T_{1c} - water inlet temperature (K);

T_{2c} - water outlet temperature (K);

T'_k - air temperature at the compressor outlet (K);

T''_k - air temperature in the cylinder at the end of filling (K);

$T(\tau)$ - the surface temperature (K);

ΔT_a - heating of the air in the cylinder (K);

ΔT_x - decrease in booster air temperature in the cooler (K);

∇T - the temperature gradient (K/m);

V - the cylinder volume (m^3);

V_d- displacement volume (m^3);

V_c - compression chamber volume (m^3);

V_h - working cylinder volume (m^3);

w - the average in-cylinder gas velocity (m/s):

X_b - the mass burned fraction;

Greek symbols:

α - air excess coefficient;

$\hat{\alpha}$ - the Seebeck tensor (V/K);

γ_r - residual gases coefficient;

δ - subsequent expansion ratio;

δ - the thickness of the material (m);

ε - compression ratio;

ε - surface emissivity;

ε_d - the valid compression ratio;

η_v - coefficient of fullness;

θ_c - the crank angle at the start of combustion (℃);

θ_{opt} - the optimal angle ℃;

λ - pressure increase ratio;

λ - thermal conductivity of the piston material (W/(m*K));

ξ - heat-availability factor;

ρ - preliminary expansion ratio;

ρ_a – air density in front of inlet valves (kg/m3);

σ - Stefan-Boltzmann constant (W/(m^2*K^4))

τ_{min} - response time;

χ - extraction coefficient;

Ψ - a share of a piston stroke;

τ - current time (s);

ω – rotation frequency (rpm).

1. INTRODUCTION

1.1. Background

Thermal-engineering experiments are based on different measurements such as temperature, heat flux, and other, for example, flow rate of moving media. But, sometimes, the measurement of the heat flux is more important and useful in different engineering applications such as industrial process control, aircraft or turbomachinery. Usually, we need to determine a big number of substance parameters, for example, thermophysical properties. There are a lot of different heat flux gages that can't perform under high heat flux and high temperature conditions in spite of a big number commercially available gages that exist in this field. But few decades, there was a significant growth in capabilities of experimenters. First of all, it is closely connected with possibility of treating signals digitally. Due to such improvement, we can provide not only visualization and archiving of the results of measurements, but we can conduct calibration of sensors and mathematical treatment of the data obtained. Of course, these improvements help researchers to change transformation part, but the variety of sensors remains almost unchangeable. Because of lack of sensors that are reliable under a certain conditions such as high temperature, temperature sensors are used much more frequently.

Since 1996, in the Laboratory of Heat Measurements of the Department of Thermal Engineering Foundations of St. Petersburg State Technical University (SPbGTU), there have been conducted a huge work to study the possibilities of heat flux sensors. Use of gradient heat flux sensor let them to get some new results that have been poorly considered by other researchers up to the present. The main results have been obtained with the use of gradient heat-flux sensors, which have been poorly known up to present. These sensors are manufactured using unique technology (Divin N. P. 1998). The distinctive feature of these sensors is a material - anisotropic monocrystal bismuth, which combines orthogonal anisotropy of thermophysical and thermoelectric properties (Sapozhnikov S. Z. 2006).

The principle of action of GHFSs is based on the transversal Seebeck effect, i.e., the appearance of thermoelectromotive force (thermo-EMF), the intensity vector of which is directed perpendicularly to the heat flux vector in a medium with anisotropy of heat conductance, electric conductance, and a thermo-EMF coefficient (Sapozhnikov S. Z. 2006). This concept had the potential to be used in a high temperature heat flux sensor.

1.2. Research problem and objectives

The main objective of the work is to consider the possibility to use Gradient Heat Flux Sensors (GHFS) to measure heat flux in the combustion chamber of compression ignited reciprocating internal combustion engines in more detail. A. Mityakov conducted an experiment, where Gradient Heat Flux Sensors was placed in four stroke diesel engine Indenor XL4D to measure heat flux in the combustion chamber. The results which were obtained from the experiment need to be compared with model's numerical output.

We will consider the example of work of piston ICE, how it is applied and what function carries out. Such issues as thermal balance of the internal combustion engine, determination of gas exchange parameters will also be included in the work.

A description of engine simulation model should be proposed, and also we need to implement a single-zone thermodynamic model of an internal combustion engine in order to compare numerical results, obtained with aid of this simulation model, and data which we get from experiment, mentioned above. The result of this implementation will be the graph of heat flux in combustion chamber in relation to the crank angle.

2. HEAT FLUX MEASUREMENT TECHNIQUES

The first law of the thermodynamic is one of the most important principles relating to the heat transfer, which states that amount of energy remains constant in any isolated system. There are three modes of the heat transfer: convection, conduction and radiation.

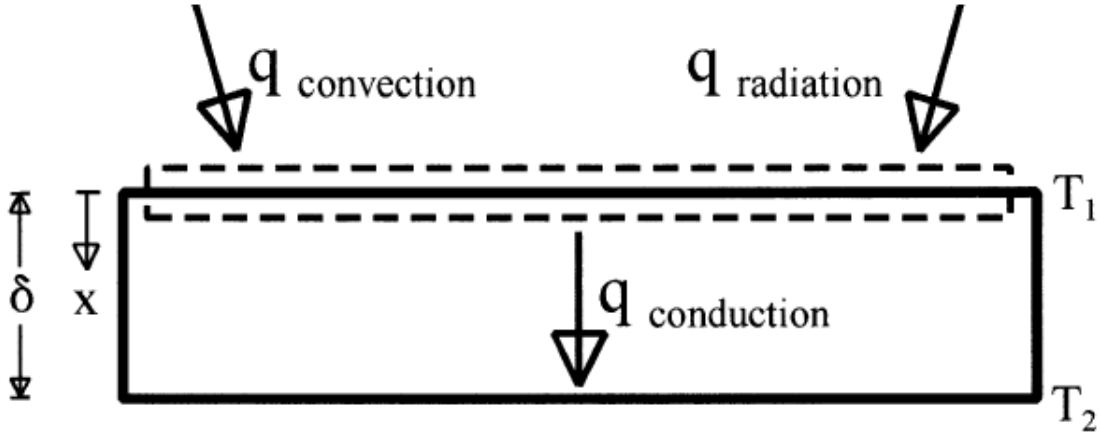

Figure 1. Energy balance.

We can write down the balance based on the first law of the thermodynamic:

$$m_{sys} C_p \frac{\partial T}{\partial t} = q_{convection} + q_{radiation} - q_{conduction}, \quad (2.1)$$

m_{sys} – mass of the system;
C_p– specific heat capacity.

It is necessary to consider all the components of the equation to have the full picture about the heat transfer and understand the principle of operation of all devices which can measure the heat flux rate.

Thermal conductivity is the transfer of heat within the same body between its parts having different temperatures. More mobile (more heated) particles of the body (molecules, atoms) transfer part of their energy in direct contact to less mobile (colder particles). Process heat conduction occurs mainly in solid substance, therefore particles are more close together with each other. So, metal sheet is heated in a single location, such as welding it, after a while, you

may find that the increased temperature and other parts of the sheet are not directly heated: heat conduction spread.

The main conduction law is a Fourier's law. It states that heat flux is proportional to the temperature gradient and it has the opposite direction.

$$\bar{q}'' = -k\bar{\nabla}T, \tag{2.2}$$

where *k* is the thermal conductivity. We have to find temperature gradient to calculate the heat flux. For a homogenous material:

$$\frac{\partial T}{\partial t} = a_{th}\left(\frac{\partial^2 T}{\partial x^2} + \frac{\partial^2 T}{\partial y^2} + \frac{\partial^2 T}{\partial z^2}\right) \tag{2.3}$$

Beside the temperature distribution, this equation has one more component - thermal diffusivity of the material.

$$a_{th} = \frac{k}{\rho C_p} \tag{2.4}$$

This method of heat flux calculation is rather complicated, if we have more than one dimension effect. The temperature distribution is linear for one-dimensional heat transfer in steady state.

$$q'' = k\frac{T_1 - T_2}{\delta}, \tag{2.5}$$

where δ is the thickness of the material.

Convection is the heat transfer in the process of moving and mixing hotter or less hot particles. This process can take place in an environment with moving particles, i.e. drip liquids and gases. Convection usually accompanied by the exchange of energy between these particles - thermal conductivity. This process is called convective heat transfer. Its intensity depends on the state, the speed and the nature of the fluid. Fluid movement can be either natural or forced. Natural (free) movement of the particles is the result of a difference in density between the hot and less hot volumes of liquid in the vessel. If a glass container with a liquid droplet is heated, you can see the rising streams of liquid. They are caused by the fact that liquid density is less than the density of its upper layers in the heated part of the liquid (bottom).

$q'' = h_T(T_r - T_s)$, (2.6)

T_r – temperature of the fluid;

T_s – surface temperature;

h_T – heat transfer coefficient.

Because of the difference in density between the hot and cold layers in accordance with the laws of hydrostatic lift occurs, under which heated particles move from the bottom up, bringing with them their energy (heat). This phenomenon is called natural convection. Simultaneously with convection some of the heat is transferred by heat conduction through direct contact between the particles of the fluid. Consequently, the phenomenon of convection causes the heat transfer in the volume of the fluid as by direct contact between the liquid particles (heat), and by moving the fluid particles in the volume at their natural movement

Thermal radiation (radiation or radiant) is the spread of heat by converting thermal energy into electromagnetic waves (radiant energy) to the heat source and the inverse transformation (absorption) in the heated body.

All bodies at any temperature emit energy that spreads through space at the speed of light in the form of electromagnetic waves, but the intensity of the radiation increases rapidly with increasing temperature.

$q'' = \varepsilon\sigma(T_w^4 - T_\infty^4)$, (2.7)

ε - surface emissivity;

σ - Stefan-Boltzmann constant ($5{,}67 * 10^{-8}[\frac{W}{m^2 * K^4}]$).

It is more usual when the heat exchange is carried out by the cumulative effects of conduction, convection and thermal radiation. Heat transfer is the complex processes of heat transfer from one fluid to another through a solid wall separating them.

Processes of heat exchange between the bodies may occur in the steady (stationary) and transient (time-dependent) modes. The temperature distribution in different areas of the body at steady state remains constant over time: the spread of heat established, and the thermal state of the

elements of the body does not change. Internal combustion engines and electric cars locomotives after a long time of work can be in the steady thermal conditions, if modes of their load and cooling conditions do not change at that time.

We can neglect the thermal radiation in the field of high enthalpy at low temperatures. If the temperature of the surface is high, so-called radiative equilibrium establishes. It means that rates of gas heating and radiation cooling are equal. And we can calculate the heat flux rate using the equation. But first of all we need to measure the surface temperature. There are a lot of different methods to determine heat flux rate with or without so-called radiative equilibrium.

2.1. Differential temperature sensors

2.1.1. One-dimensional planar sensors

The one-dimensional heat flux is inversely proportional to the thickness of the sensor δ and directly proportional to the thermal conductivity of the sensor k and to the temperature difference:

$$q'' = \frac{\delta}{k}(T_1 - T_2) \tag{2.8}$$

The thickness of the sensor d and thermal conductivity k are not known with sufficient accuracy for any particular sensor to preclude direct calibrations of each sensor (Diller T. E. 1999). Considering the one-dimensional heat flux in terms of location in space, we can say that it perpendicular to the surface. In some cases we have problems to attach sensors to the surface, that's why we usually use adhesive layer between sensor and surface. But it is not a positive factor for calculation of the heat flux, because we have to consider the additional thermal resistance of the layer which can be the cause of thermal disruption. Of course, to get figures of temperature differences in appropriate way we need to quantify this disruption, otherwise our calculations will be less accurate.

In spite of big number of methods, the easiest way to measure the temperature difference is use of the thermocouples. The principle of operation of the thermocouples is rather simple. The voltage output, E, is directly proportional to the temperature difference:

$$E = S_T(T_1 - T_2), \tag{2.9}$$

where S_T is the Seebeck coefficient or thermoelectric sensitivity of the material. To enhance the voltage output from a temperature difference, thermocouples can be connected to form of thermopile. It is usually necessary, because a single thermocouple doesn't produce enough output voltage. So the equation 2.9 can be transformed in following equation:

$$E = NS_T(T_1 - T_2), \tag{2.10}$$

where *N* is a number of thermocouple junction pairs.

Thermoelectric sensitivity of the heat flux is:

$$S = \frac{E}{q''} = \frac{NS_T\delta}{k} \tag{2.11}$$

The main way to determine the sensitivity is the direct calibration, however, parameters which make up equation can be used to determine effects for design purposes.

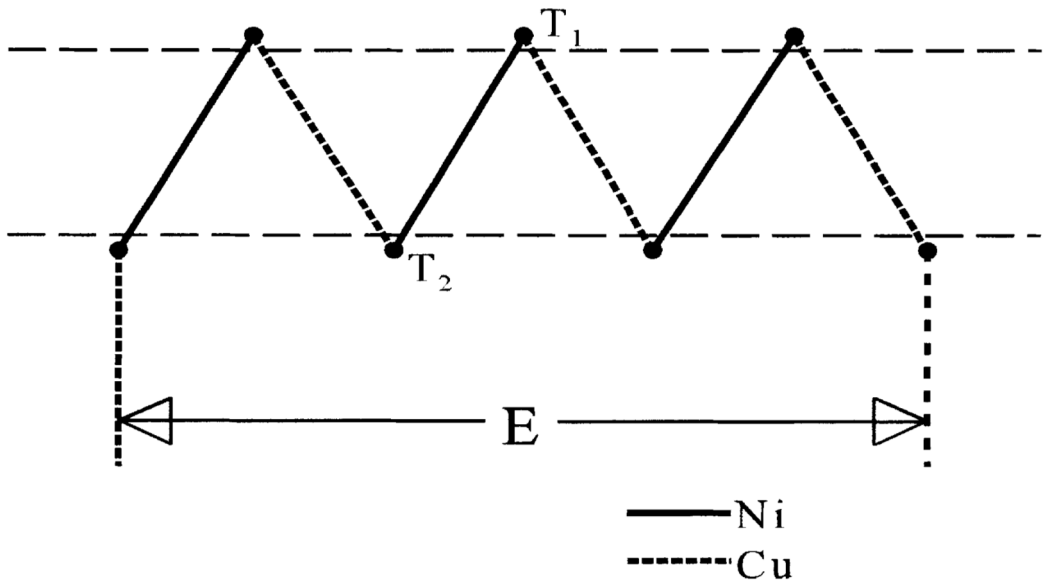

Figure 2. Thermopile for differential temperature measurement (Diller T. E. 1993).

One of the currently existing applications is a thermopile described by Ortolano and Hines (Ortolano D. J. et al. 1983). For the record, it is still manufactured by one of biggest company in this field, Rdf Corp. The technology is illustrated on the figure 3.

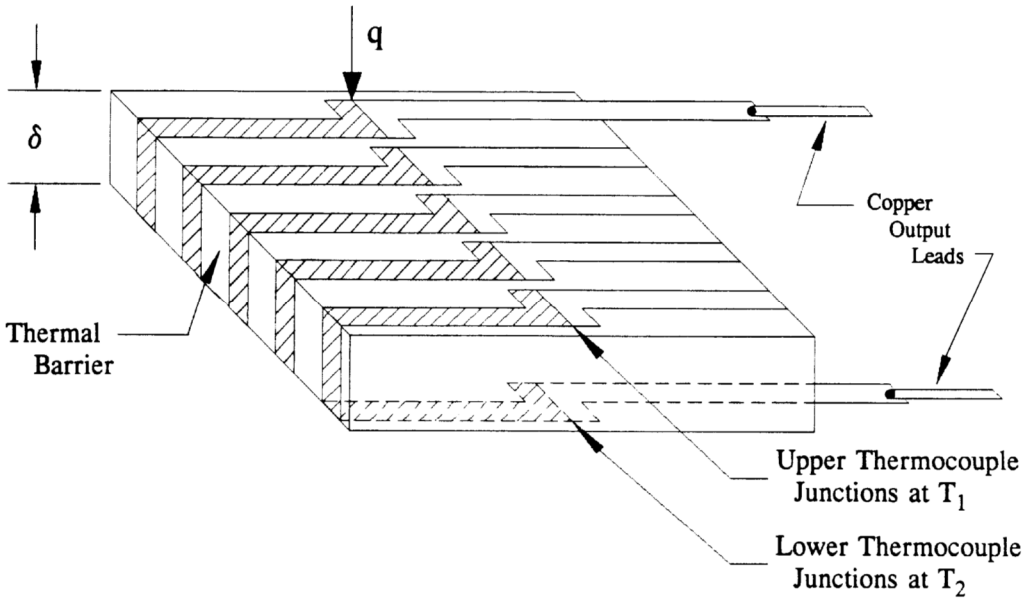

Figure 3. Thermopile heat flux sensor (Ortolano D. J. et al. 1983).

I would like to give some information about this technology. Thin pieces of two types of metal foil are alternately wrapped around a thin plastic (Kapton) sheet and butt-welded on either side to form thermocouple junctions (Diller T. E. 1999). It is also necessary to have one more thermocouple in order to provide measurement of sensor temperature. Considering the parameters of the thermopile, I'd like to mention the following parameters and properties:

1) It is used in industrial and research application.
2) Limited to temperatures below 250 °C
3) Limited to heat fluxes (100 kW*m–2).
4) Fast time response (20 ms).
5) Micro-foil sensors can be used in a different number of surface shapes.

The application is manufactured by International Thermal Instrument Co. and has a similar design with application mentioned above. The main difference in construction is welded wire about 1 mm which is used to form thermopile. The place of this wire is across a sensor. Such add to design allow manufacture raise the sensitivity and upper temperature limit by 50 °C in comparison with application of Rdf. Corp. Also, this application is usually used in buildings and physiology.

Much thinner sensor was developed by Vattel Corp. and was called Heat Flux Microsensor. It has a similar technique, I mean, based on spatial temperature gradient. In contrast to the other

applications it has two thin-film less than 2 microns deposited on the substrate of the aluminium nitride. Such thickness allow manufacture reduce time response almost in two times (10 microseconds) in comparison with other manufactures. Temperature resistor (RTS) is also used in this application. The principle of operation is not so complicated. We need to determine the temperature and if we want to do it, first of all, we should measure the resulting voltage. For this we need to pass a not big constant current through the resistance. Furthermore, if we need to know what kind of change in properties of the material might happen with change of the temperature or we would like to check the calibration of the microsensor or, at last, we want to determine heat transfer coefficient, we have to know also a substrate temperature. The high operational temperature (it can exceed 800 °C) and very fast time response are very useful factors in some aerodynamic applications or in engines with combustion flows and many other applications.

One more application manufactured by Vattel Corp. was described by Terrel (Terrell J. P. 1996) as an application with a similar design with Heat Flux Microsensor, but, of course, it has some differences. There is a dielectric inc which is used for the thermal resistance layer and it works with a pair of thermocouple which are made of copper and nickel. In spite of rather high thickness of the materials (approximately 350 microns), the thermal resistance is not proportional to the thickness and rather low. This fact has a clear explanation, all materials have a high thermal resistance. There are some properties of the application:

1) Due to a big number of connected thermocouples (approximately 10000 pairs), sensitivities are sufficient to measure heat fluxes as low as 0,1 W*m–2 (Diller T. E., 1999)
3) Limited to temperature below 150 °C.
4) It is used in building, biomedicine, fire detection and in other sphere of life.

One more technique based on spatial temperature gradient was described by Hauser (Hauser R. L. 1985) and a review is given by van der Graaf (Van der Graaf F. 1989). The main idea is to wrap wire and then plate one side of it with a different metal (Diller T. E. 1999). Constantan and copper are usually used as the main materials. So we have wire made of constantan which is placed all around the application in comparison with other sensors where wire forms discrete thermocouple junction. The main advantage of this application is a rather small cost. There are two manufactures, Concept Engineering and Thermonetics which are the main producer of such devices.

Concept engineering sensor:

1) Sensitivity to the heat flux is high (because of a big number of windings).
2) Thermal resistance is high.
3) Time constant is 1 s.
4) Limited to temperature below 150 °C.

Thermonetics sensor:

1) Thickness is rather high (between 0,5 mm and 3 mm).
2) Time constant is more than 20 s.
3) Limited to temperature below 200 °C (for exception, ceramic units, where the temperature is limited to 200 °C).
4) The spheres of use are building structure, medicine, geothermal and others.

One more application known as a Schmidt-Boelter gage was discussed by Neumann (Neumann D., 1989) in terms of aerodynamic. And also Kidd (Kidd C. T. et al. 1995) conducted some analyses in order to determine the effect of the piece of aluminum on heat flux. The main manufacture of Schmidt-Boelter gage is Medtherm Corp.

2.1.2. **Gardon gage**

This technique was originated by Robert Gardon (Gardon R. 1953) in order to have an opportunity to measure radiation heat transfer. The circular foil or Gardon gage consists of a hollow cylinder of one thermocouple material with a thin foil of a second thermocouple material attached to one end (Diller T. E. 1999). There are two thermoelectric materials this Gardon gage made of. The first thermoelectric material is usually constantan and it is a basic material for the metallic foil. The second thermoelectric material is copper and heat sink and differential thermocouple wires made of copper. As mentioned, we have differential thermocouple. We can achieve it by attaching of the wire in the center of the metallic foil. The main task is to measure temperature difference between the center and the edge of foil.

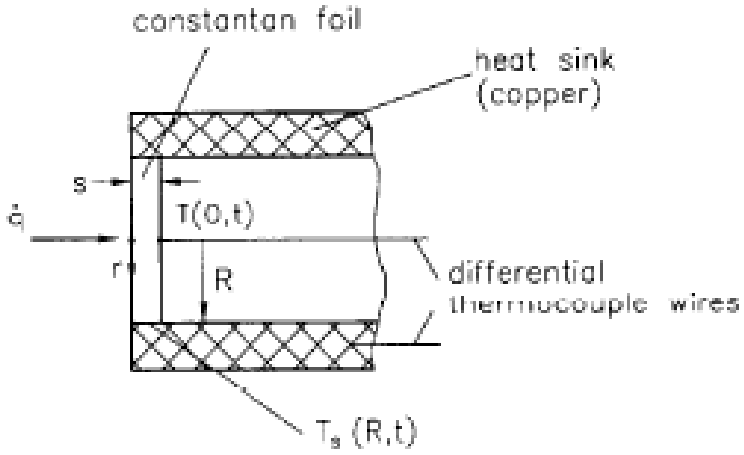

Figure 4. Principal scheme of Gardon gauge (Giilhan A. 2007).

We can describe the process of heat conduction in radial direction using the polar co-ordinates:

$$\frac{\rho C_p}{K}\frac{\partial T}{\partial y} = \frac{1}{r}\frac{\partial T}{\partial r} + \frac{\partial^2 T}{\partial T^2} + \frac{\dot{q}}{sK}, \tag{2.12}$$

where *s* is the thickness of the foil, *R* is an active radius of the foil.

Write down the boundary conditions:

$T(r,0) = T_s$ at $0 < r < R$

And

$T(R,t) = T_s$ for $0 < t < \infty$

We can solve equation using the boundary conditions and we get:

$$\dot{q} = \frac{4sK^{\cdot}}{(R^2 - r^2)}(T - T_s) \tag{2.13}$$

So, if we want to calculate the heat flux in the center of the foil (r=0), neglecting heat losses down the center wire, we get:

$$\dot{q} = \frac{4sK}{R^2}(T - T_s) \tag{2.14}$$

As we can see heat flux is directly proportional to the temperature difference. Copper-constantan thermocouple pair is used to measure temperature difference between center and the edge of the foil.

There are two main manufactures of this kind of application, Medtherm and Vatell, which sell their devices for rather moderate cost. One of the most important application of the Gardon gages is measurement of the heat flux in some industries to check the flammability of materials. But in spite of rather simple and rugged construction, it has some problems it is needed to work with convective heat transfer. The main reason of this is that output is incorrect for convective heat transfer because of the distortion of the temperature profile in the foil from the assumed radially symmetric, parabolic profile of radiation (Kuo C. H. et al. 1991). The only decision of this problem is to try to follow temperature difference and keep it across the gage.

One of the main condition of the reliable operation of the Gardon gage is to prevent exceeding of the temperature over the limit. To avoid such exceeding and to provide normal operating condition, manufacture uses the water cooling system. It means that water goes through the body of the sensor and keeps the system on acceptable level. It is necessary in high heat flux situations such as combustion. Because of the resulting temperature mismatch of the gage and surrounding material in which it is mounted, a water-cooled gage is not recommended for convection heat transfer measurements (Diller T. E. 1999). It is necessary to understand that there should not be any condensation on the sensor face.

The measurement of the heat flux by Gardon gage is not the only opportunity to use it. It can be used for separation of convection from radiation. One of the most famous way to separate them is to use transparent window. We need to put it over the sensor to eliminate the convection. That's why we can call it radiometer. But some situations can interrupt the working process of the radiometer. For example, if there any dirty environment near the window, the operational functions of the window can be disturbed. To solve this problem manufactures take the particles away by air blown across the sensor face. This technique is used by all manufactures in in high-ash boilers and gas turbine combustors.

2.2. Semi-infinite surface temperature methods

The principle of this method is to measure surface temperature on a test object, which can be considered to be a semi-infinite solid. It means that for rather thick material and short enough times we can assume that the transfer of heat is one-dimensional and the conductive heating does not reach the back surface of the material. It can be assumed that the surface temperature doesn't change within the period of time.

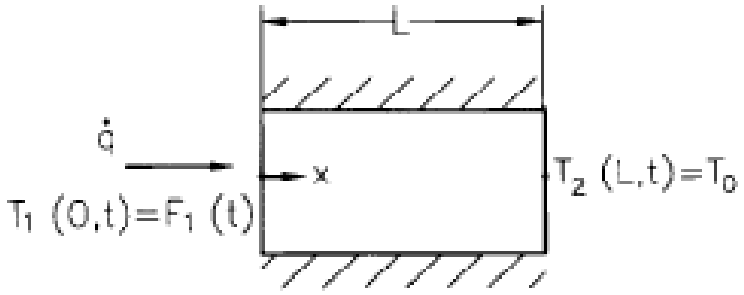

Figure 5. Boundary temperatures of the semi-infinite models.

First of all, consider the equation for one-dimensional heat flux:

$$\frac{\partial T}{\partial t} = \frac{K}{\rho C_p}\frac{\partial^2 T}{\partial x^2} \tag{2.15}$$

Write down the boundary conditions for this model:

$T(0,t) = F_1(t) = T(t)$;

$\dot{q}_s(t) = K(\frac{\partial F_1(t)}{\partial x})_{x=0} = K(\frac{\partial T(t)}{\partial x})_{x=0}$;

$T9L,t) = T(\infty,t) = T_0$.

Now, we can get the solution of the equation for one-dimensional heat flux based on the boundary conditions for the heat flux rate to the semi-infinite probe:

$$\dot{q}(t) = \sqrt{\frac{\rho C_p K}{\pi}}\left[\frac{T(t)}{\sqrt{t}} + \frac{1}{2}\int_0^t \frac{T(t)-T(\tau)}{(t-\tau)^{\frac{3}{2}}}d\tau\right] \tag{2.16}$$

Rewrite this equation for the constant heat flux rate:

$$\dot{q} = \frac{\sqrt{\pi}}{2}\sqrt{\frac{\rho C_p K}{t}}[T(0,t) - T_0] \tag{2.17}$$

$T(0,t)$ is surface temperature as a function of time, T_0 is an initial temperature.

To recreate a heat flux signals we can use several methods, but the simplest one is to use the analytical solution with each sampled data point (Diller T. E. 1999). Cook and Felderman (Cook W. J. et al. 1966) presented an equation which let us understand this conversion:

$$q''(t_n) = \frac{2\sqrt{kpC}}{\sqrt{\pi\Delta t}}\sum_{j=1}^{n}\frac{T_j - T_{j-1}}{\sqrt{n-j}+\sqrt{n=1-j}} \tag{2.18}$$

Modifications are also available to provide more solution stability (Diller T. E. et al. 1997). More complex techniques include the use of parameter estimation techniques (Walker D. G. et al. 1995) and numerical solutions to account for changes in property values with the changing temperature (George W. K. et al. 1991). Because of the noise amplification inherent in the conversion from temperature to heat flux, analog methods have been developed to convert the temperature signal electronically before digitizing the signal (Schultz D. L. et al. 1973).

There are two big categories for the measurement of the surface temperature and following determination of the heat flux. The first category is a point measurement where thermocouples are used, and the second is an optical methods. Of course, to use any of these methods we need to start test procedure and reduce data as much as possible. Let's consider all categories in detail. The thin-film gauge is one way to determine heat flux and relates to the first category – point temperature measurements. Aluminum film is usually used in this technique. There are different ways to attach the film to the substrate, for example, painting and vacuum deposition. The main manufactures of substrate are Pyrex, fused Quarts or MACOR.

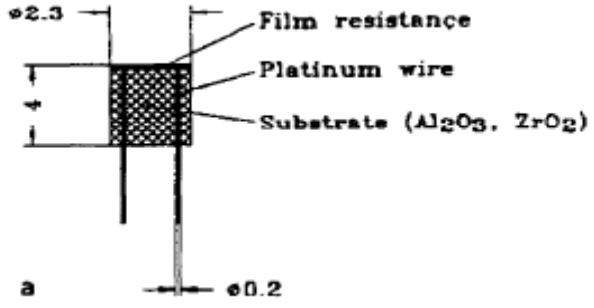

Figure 6. Thin-film gauge of RWTH Aachen (Simeonides G. et al. 1993)

This device developed in the RWTH Aachen has an almost ideal output signal. The manufacture reached such data because of high temperature-resistance coefficient. There are some properties of this device:

1) Thickness of the sensor is several nanometers.
2) The response time is very short (no more than 1μs).
3) Sensor is very sensitive even to small particles.
4) Sensor is used in the aerothermodynamic applications, internal combustion engines, gas-turbine engines and etc.

Point temperature measurements are often made with coaxial surface thermocouple. The main principle of the application is similar with the previous device – to determine the surface temperature of a body as we assumed as semi-infinite surface. The design of the device is not so complicated. It has thermocouple material, inside which there are thermocouple wire and insulating layer between them.

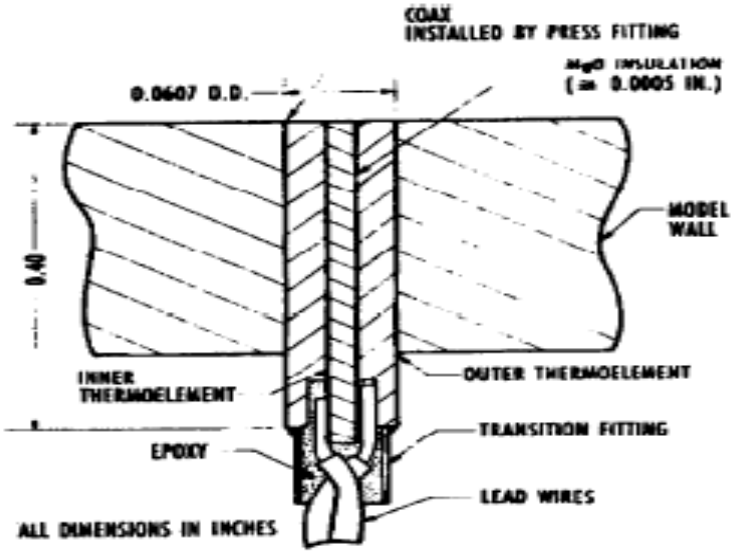

Figure 7. Sketch of the coaxial surface thermocouple.

The coaxial thermocouple assembly is completed by attaching thermocouple lead wires to the coaxial thermoelements (Simeonides G. et al. 1993). We need to measure the surface temperature to determine the heat flux by the equation 2.8. It can be used short and long wind tunnels. Medtherm Corp. is one of the main manufacture of the coaxial surface thermocouple. There are some advantages of this method:

1) Fast response time (approximately 50 μs)

2) Good durability.

3) No calibration is required because of self-generating.

And disadvantages:

1) Weak output signal.

2) Complex data reduction.

One more method of point temperature measurements is null-point calorimeter. It was developed by AEDC. Now, the main manufacture is also Medtherm Corp. And it is used for quite big heat flux (over 1000 kW m–2).

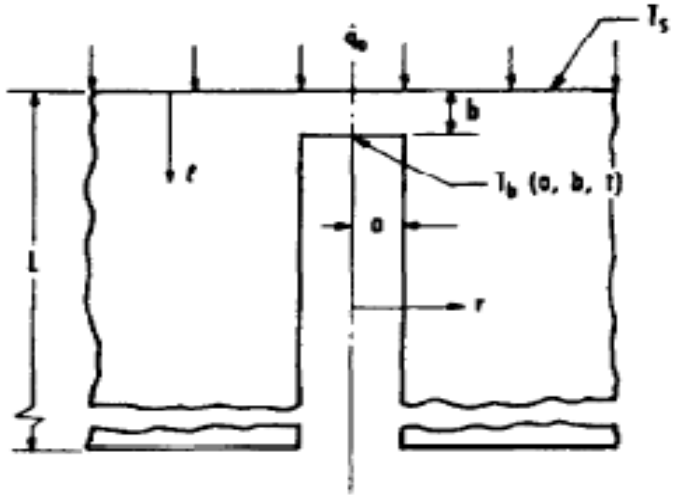

Figure 8. Concept of the null-point calorimeter.

If we look on the centerline of the cylinder cavity, we can see the point (0,b). It is a null point. So, we assumed that measured temperature development in this point is identical to the surface temperature history on the outside surface of the same thermal mass without cavity (Giilhan A. 2007). Detailed thermal analysis was conducted to be sure that this assumption is right. So, according to the analysis, if the ratio of the hole radius to the axial distance is approximately 1,4, then we can assume that temperature in the null-point is almost similar with surface temperature history. As a result of this assumption, we can determine heat flux ratio by inserting measured temperature in the equation 2.8. Need to say that we use Chromel-Alumel thermocouple to measure the temperature in the null-point. Thermocouples and wires mounted in a cavity behind the cylinder. It is necessary in order to protect them.

Optical methods allow us to obtain visual representation of the distribution of the temperature over the surface to the greater extent than quantitative heat flux value. Due to the calculations of the heat flux is too complicated because of much data can be collected, we can't determine heat flux with pinpoint accuracy. In spite of this fact, these methods are very popular. Let's consider some optical methods to have a full picture about semi-infinite surface temperature methods.

One of the optical methods is based on using liquid crystals. The main idea of this method is to record color change of the specially prepared molecules, which change their color depending on the temperature. Usually the range of temperature is not so big and the figures are approximately between 25 ℃ and 45℃. But one of the manufactures of this technology, Hallcrest, achieved expansion of the range. Their devices can work with temperature range from 5 ℃ and 150℃. They can easily be spray-painted onto a blackened surface for testing. Setting the lighting for reproducible color, temperature calibration, image acquisition, and accurately establishing the starting temperature are crucial steps (Diller T. E. 1999). There is a one problem. In spite of rather low cost of the basic material, equipment for temperature measurement is quite expensive. There are a lot of companies on the market which produce different equipment such as high-quality video camera, calibration system, software for image processing and other equipment. The main manufacture in this field is Image Therm Engineering.

As we have already discussed for radiation heat transfer, surface temperature can be closely connected with radiation which is emitted by all surfaces. The advent of high-speed infrared scanning radiometers has made it feasible to record the transient temperature field for determination of the heat flux distribution (Simeonides G. et al. 1993). We also need to find the radiation field in order to have dependence between surface temperature and radiation emission. The main problem is a cost of equipment. To have camera and other necessary equipment, company or institute should have decent monetary funds.

Thermographic phosphors emit radiation in the visible spectrum when illuminated with ultraviolet light (Diller T. E. 1999). There is the dependence between surface temperature and intensity of emissions. But most of technologies in this sphere are under development now. So, there a lot of expensive equipment needed to record the transient optical images. Also, manufacturing companies have some problems with calibration of the devices.

2.3. Calorimetric sensors

2.3.1. Thin-skin technique

The main principle of the thin-skin technique is the measurement of the slope of the back surface temperature history. All devices of this technique are made of thin metals and also they have thermocouples on the back surface. One of the properties of such devices is a constant temperature throughout the material, but it can change value with position around the model. And also in most cases the temperature varies with time. We can calculate the heat flux rate with help of rather simple equation:

$$\dot{q} = \rho C_p s \frac{dT}{dt}, \tag{2.19}$$

where *s* is the thickness of the wall.

Some important assumptions and properties relating to the thin-skin technique:

1) We can neglect the heat conduction to the other structures during the measurement.
2) Heat flux rate and properties of the material have a big impact on working time of the sensor.
3) Simple data reduction.

There are some errors need to be solved or avoided:

1) Lateral conduction along the surface material (Moffat R. J. 1990).
2) Heat loss by conduction down the thermocouple wires (Diller T. E. 1993).
3) Heat loss from the back surface, which is usually considered adiabatic (Ortolano D. J. et al. 1983).

In spite of the fact, that all devices of the thin-skin technique are very expensive as well as optical models, there are a lot of modes which are implemented for the modern aerodynamic testing.

2.3.2. Slug calorimeter

The principle of the slug calorimeter work is based on the calculations of the amount of heat is being stored during the measuring time. There are three main parts of the calorimeter: thermocouples; calorimetric mass, which is usually in form of metallic disk; thermal insulator. One of the main problems is to avoid radial heat losses. The decision of the problem was founded and the main idea is to integrate the slug into the thermal insulator. We can see the sketch of the slug calorimeter on the figure:

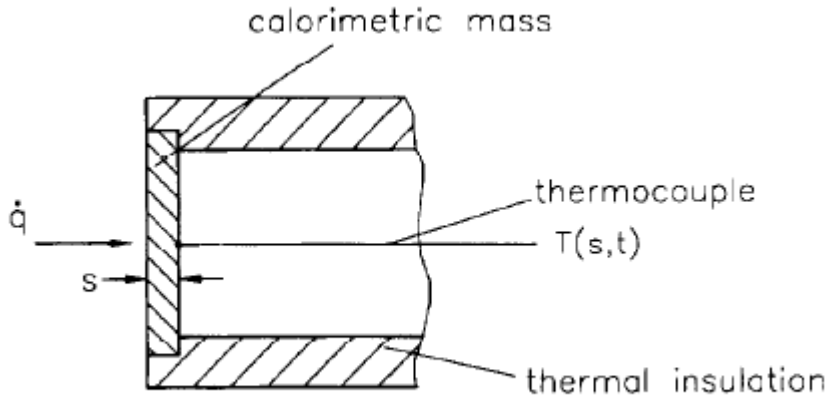

Figure 9. Sketch of slug calorimeter.

As for thin-skin technique, the heat flux rate can be calculated with help of the equation. But first of all we have to measure the temperature on the backside of the metallic disk. It is assumed that temperature throughout the sensor is uniform and we can write down the equation for the temperature change:

$$\frac{T-T_r}{T_i-T_r} = e^{-t/\tau}, \tag{2.20}$$

where T_i is the initial temperature, contact with the liquid occurs at temperature T_r.
Time constant can be calculated by following equation:

$$\tau = \frac{mC_p}{h_T A_{ac}}, \tag{2.21}$$

where A_{ac} is the active surface, h_T is the heat transfer coefficient. So we can calculate the heat transfer coefficient as long as we find the time constant. We can find it from the temperature response. In spite of rather simple construction, there are some disadvantages of this model:

1) High level of the heat losses.
2) Non-uniform distribution of the temperature profile.

There were some researches to develop more useful device in comparison with slug calorimeter. Not so long ago plug-type heat flux gage was developed by Liebert. It has four thermocouples. There are some advantages of this model in comparison previous models:

1) It can estimate not only the temperature gradient, but it also can follow the thermal energy content.
2) Better heat flux estimation.
3) Undisturbed measurement surface.

2.3.3. Water-cooled calorimeter

There is another calorimeter to measure the heat flux rate. It was developed in the Institute of Mechanical Problems (IPM) in Moscow. The heat flux rate is measured in the steady state flow. The main idea is to measure the quantity of the heat absorbed by cooling water. The side heat appears on the back surface of the cylinder and cooling water is necessary to remove it.

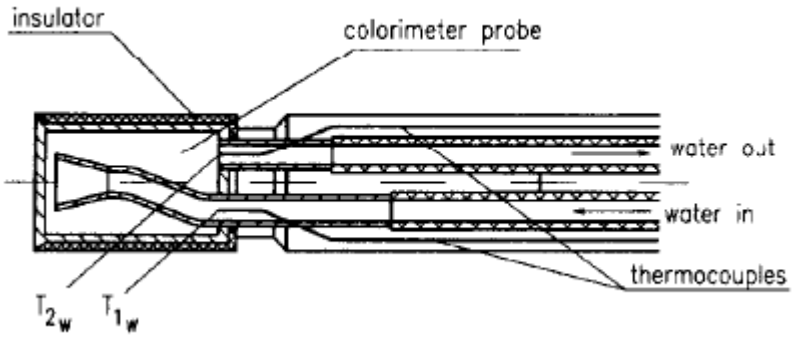

Figure 10. Sketch of the water-cooled calorimeter.

The heat flux can be calculated with help of following equation:

$$\dot{q} = \frac{\dot{m}_c C_{pc}(T_{2c} - T_{1c})}{A}, \tag{2.22}$$

A - cross section area of the probe;

C_{pc} - specific heat of water;

T_{2c} - water outlet temperature;

T_{1c} - water inlet temperature;

$\dot{m}_c$ – water mass flow rate.

There are a lot of manufactures of the calorimeter probes working on the IPM-principle. For example, DLR manufactured water cooled calorimeter probe which is rather widespread for heat flux measurement.

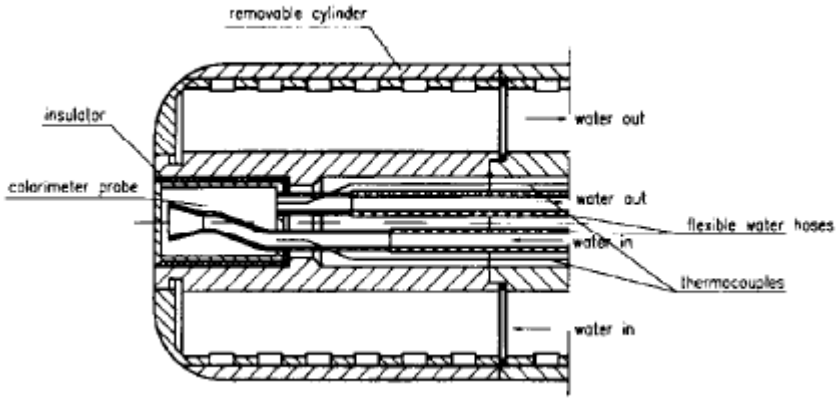

Figure 11. Water-cooled calorimeter probe of DLR.

Table 1. Heat flux instrumentation.

Manufacturer	Sensor	Description	Approximate price, (U.S.$)
RdF	Micro-foil	Foil thermopile	$100
Vatell	HFM	Microsensor thermopile	$900
Vatell	Episensor	Thermopile	$100–250
Concept	Heat flow sensor	Wire-wound thermopile	$100–300
Thermonetics	Heat flux transducer	Wire-wound thermopile	$50–900
ITI	Thermal flux meter	Thermopile	$150–350
Vatell	Gardon gage	Circular foil design	$250–500
Medtherm	Gardon gage	Circular foil design	$400–800
Medtherm	Schmidt-Boelter	Wire-wound thermopile	$500–800
Medtherm	Coaxial thermocouple	Transient temperature	$250–450
Medtherm	Null-point calorimeter	Transient temperature	$650–800
Hallcrest	Liquid crystals	Temperature measurement kit	$200
Image Therm Eng.	TempVIEW	Liquid crystal thermal system	$30k–50k

2.4. Gradient heat flux sensors.

There are a lot of different types of heat flux sensors (HFS). Most of them are the heat flux sensors which upper temperature level is approximately 300 – 500 K. That's why it is impossible to use them for high temperature measurements. For example it cannot be used in aircraft industry or power engineering. But the new generation of the HFS is the artificial anisotropic thermoelements. Such elements are usually produced from metal or alloys, but it is also can be produced from semi-conductors.

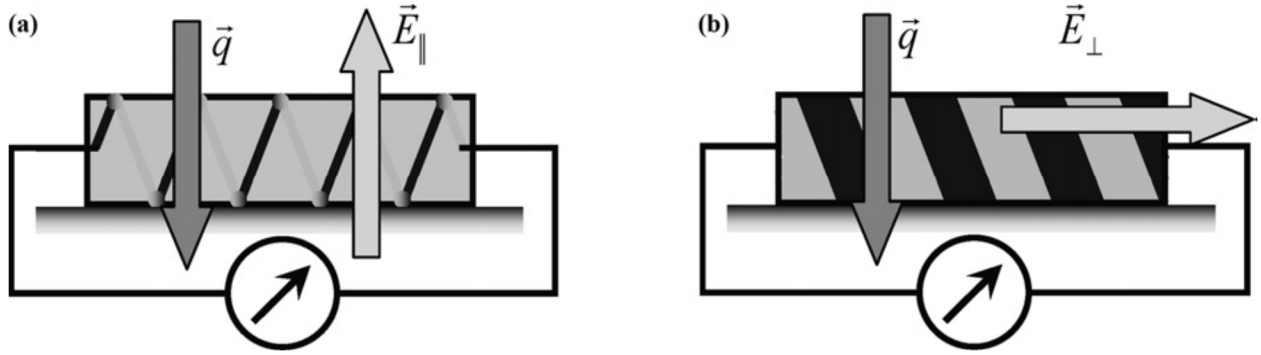

Figure 12. Thermocouple and anisotropic HFS.

In present day the auxiliary-wall-type HFSs are the plates with differential thermocouple junctions inserted at their surfaces (Pullins C. A. et al. 2010). The heat flux $\vec{q}$ and electric vectors field E_T are collinear in such thermocouple as we can see on the figure 12(a).

On the figure 12(b) we can see the anisotropic heat flux sensor, where electric vectors field E_T is normal to the heat flux $\vec{q}$. The principle of anisotropy is creation of the temperature gradient in two directions. We can oversee the temperature gradient across and along of the heat flux. Such effect was called transverse Seebeck effect. Heat flux sensors based on the anisotropic thermoelements have such properties of the material as anisotropy of thermal conductivity; electric conductivity and thermoelectromotive force (thermo-EMF) (Mityakov A. V. et al. 2011).

Because these sensors generate output signal proportional to transversal temperature gradient which is proportional to along temperature gradient which in turn is proportional to an applied heat flux, we named it as gradient heat flux sensors (GHFS) (Sapozhnikov S.Z. et al. 2003).

As we know, there are not many materials which can be used for anisotropic thermoelements. One of such material is bismuth single crystal.

One of the main properties of heat flux sensors based on the artificial anisotropic thermoelements is a very small response time generated in the layer of the sensor. It is usually in the range of $10^{-8} - 10^{-9}$ s.

2.4.1. Fundamentals of the GHFS

According to the tensorial description of the Seebeck effect the electric field vector E_T is (Balagurov B.Ya 1968):

$$E_T = -\hat{\alpha} * \nabla T, \tag{2.23}$$

where $\hat{\alpha}$ (V/K) is the Seebeck tensor and ∇T (K/m) is the temperature gradient.

Sensitivity S_0 (V/W) of the artificial anisotropic thermoelement is (Snarskii A.A. et al. 1997):

$$S_0 = \frac{e}{q_z * A_{an}}, \tag{2.24}$$

e – thermo – EMF (V);

q_z – heat flux per unit area (W/m2);

A_{an} – anisotropic thermoelement's area (m2).

The maximal sensitivity $S_{0max} = S_0(\theta_{opt})$ can be reached with the angle θ_{opt}.

$$\theta_{opt} = \pm arctg\sqrt{\frac{k_{xx}}{k_{zz}}}, \tag{2.25}$$

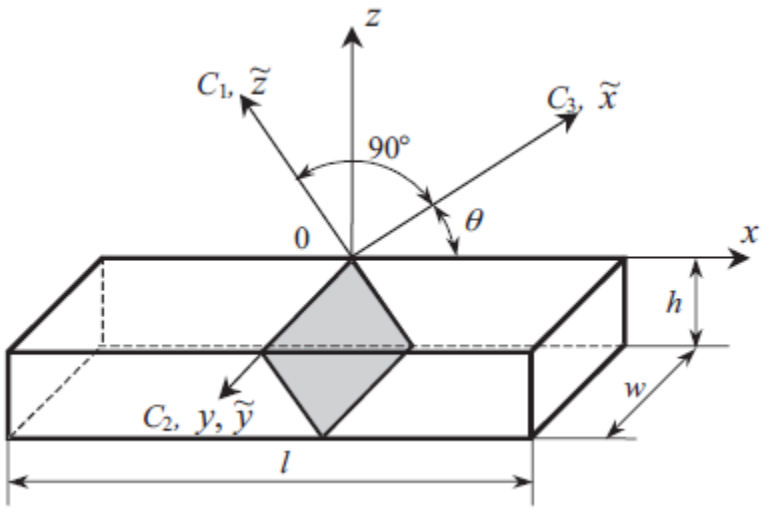

Figure 13. Anisotropic thermoelement.

l × w × h – sensor dimensions;

C1, C2, C3 – crystallographic axes;

$\tilde{x}, \tilde{y}, \tilde{z}$ – crystal coordinate axes;

x, y, z – laboratory coordinate axes;

k_{xx}, k_{zz}- components of the thermal conductivity tensors.

It is most usual to use batteries of connected anisotropic thermoelements because of small output signal.

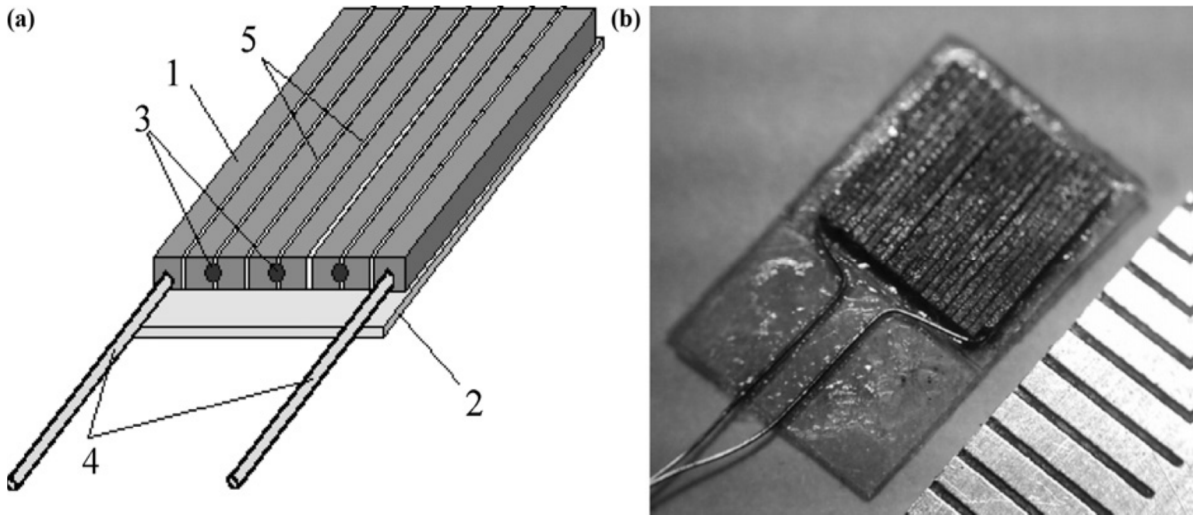

Figure 14. Schematic (a) and general view (b) of a battery GHFS (Divin N. P. 1998), (next to mm scale). The figures are used to denote: 1 – AT; 2 – mica substrate; 3 – pure bismuth soldering junctions for electrical connection between ATs; 4 – current leads; 5 – teflon or mica insulation gaskets.

There is also another heat flux sensor based on artificial anisotropic media. It is also known as heterogeneous gradient heat flux sensors (HGHFS).

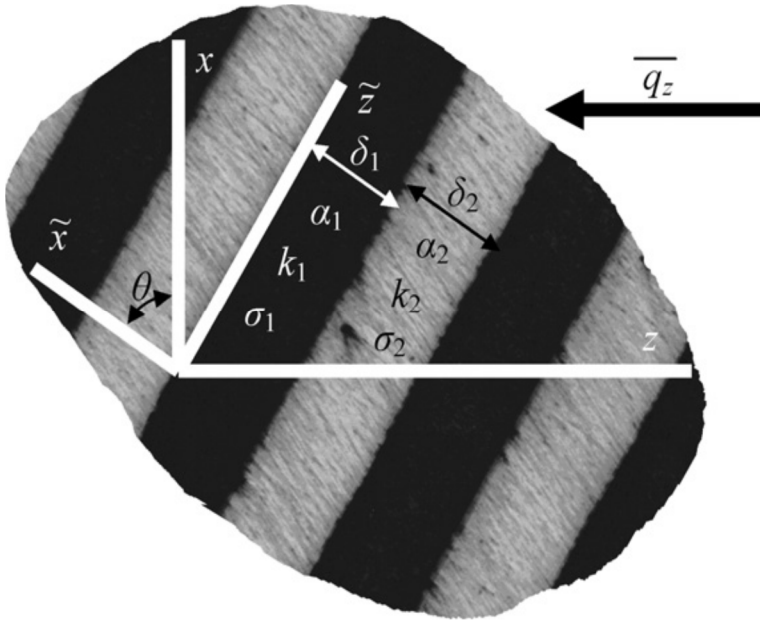

Figure 15. Layered composite used for creation of heterogeneous gradient heat flux sensors.

Optimal angle θ_{opt}:

$$\theta_{opt} = \pm arctg \frac{1+K_\delta}{\sqrt{\left(1+\left(\frac{K_\delta}{K_k}\right)\right)(1+K_\delta K_k)}}, \quad (2.26)$$

$K_k = k_2/k_1$ – dimensionless value for thermal conductivity;
$K_\sigma = \sigma_2/\sigma_1$ – dimensionless value for electric conductivity;
$K_\delta = \delta_2/\delta_1$ – layers thickness ratio.

2.4.2. Sensors design and construction

There are a lot of different constructions of the heat flux sensors. One of them was elaborated A. F. Ioffe in Physics and Technical Institute. The sensing element was based on $MnSn_{1.7}$. It was in form of plate with the optimal angle $\theta_{opt} = 45$℃ towards the crystallographic axis C_1. The response time of such sensor is approximately $10^{-11} - 10^{-13}$.

Anisotropic thermoelement of cadmium antimonide (CdSb) can be used in radiation detector instead of several hundred of copper – constantan thermocouples. The main properties of this sensor:

1) Receiving pad is made from copper (0,02 mm) and covered by camphoric niello.
2) The size of each section of the receiving element - 14 mm long, 1,2 mm wide and 0,3 mm thick.
3) Electric resistance is 2–3 kΩ.
4) Sensitivity is 150 mV/W.

Another application of the heat flux sensor is based on the single crystal of bismuth 0.9999 pure. It was created by Divin (Divin N. P. 1998). And there are some main properties of the sensor:

1) Volt–watt sensitivity S_0 = 5–65 mV/W.
2) Response time $\tau_{min} \approx 10^{-9}$s.
3) Temperature range is 20 – 544 K.

Slanted – layer sensor was made At the Polytechnic Institute of Virginia State (USA) (Sujay R.-M. 2005). This sensor consists of 46 alternating layers of steel and brass. It has low sensitivity level (approximately $3(\frac{W}{cm^2})$) and the angle $\theta_{opt} = 45℃$. One more sensor was constructed to operate at high temperature conditions. It has five steel and six brass layers and was called "straight-layered".

FORTECH HTS GmbH company made ALTP (Atomic Layer Thermo Pile) sensor (Knauss H. et al. 2006) which is based on the transverse Seebeck effect. It showed good results in the laser radiation experiments.

In 2007 in Saint-Petersburg State Polytechnical University we have created gradient sensors based on layered metal, alloys and semiconductor composites (Sapozhnikov S.Z. et al. 2003). Composition of stainless steel (18% Cr, 9% Ni, 2% Mn, 0.8% Ti) + nickel, steel (13% Cr) + nickel, chromel + alumel and iron + constantan was created to achieve upper temperature level of 1300K (Sapozhnikov S.Z. et al. 2007).

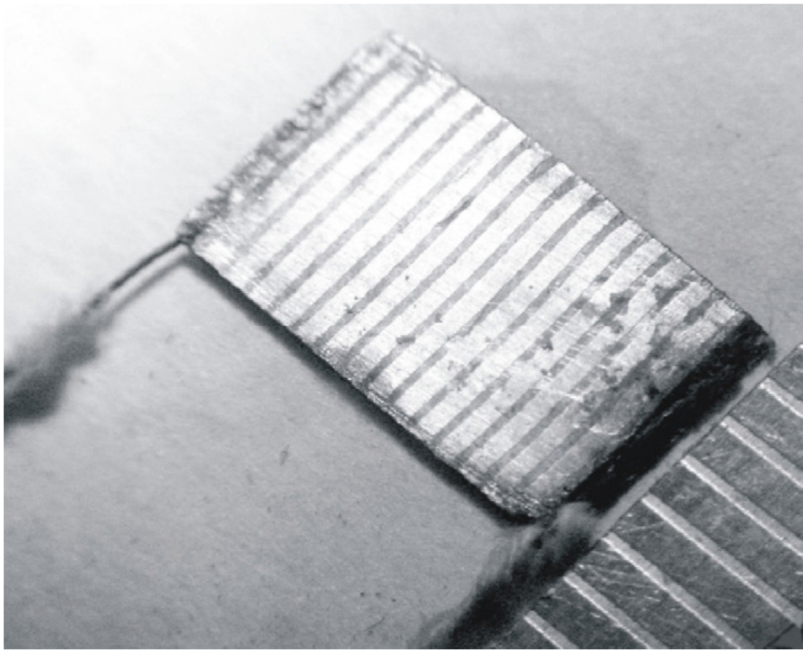

Figure 16. HGHFS made from steel + nickel (scale in mm).

In the table we can see volt–watt sensitivity of heterogeneous gradient HFS at temperature about 300 K.

Table 2. Volt–watt sensitivity of heterogeneous gradient HFS at temperature about 300 K.

Composition	Volt–watt sensitivity (mV/W)
Nickel + steel	0,40
Chromel + alumel	0,35
Titanium + molybdenum	0,02

3. MEASUREMENTS AND CALCULATIONS OF THE INTERNAL COMBUSTION ENGINE

Thermal expansion is applied in an internal combustion engine (ICE). We will consider on an example of work of piston ICE how it is applied and what function carries out. The power machine, which can transform any energy in mechanical work, is called as the engine. Engines, in which mechanical work is created as a result of transformation of thermal energy, are called as thermal. Thermal energy turns out when burning any fuel. The thermal engine, in which the part of chemical energy of the fuel, which is burning down in a working cavity, will be transformed to mechanical energy, is called as a piston internal combustion engine.

3.1. ICE classification

The greatest distribution of ICE was as power installations of cars, in which process of combustion of fuel occurs of with extraction heat and its transformation into mechanical work directly in cylinders. But in the majority of modern cars internal combustion engines, which are classified in different ways, are established: on a way of the atomization of fuel - engines with an external atomization of fuel at which gas mixture prepares out of cylinders (carburetor and gas), and engines with an internal atomization of fuel (the working mix is formed in cylinders) - diesel engines; on a way of implementation of a working cycle - four-cycle and duple; on number of cylinders - one-cylinder, two-cylinder and multicylinder; on an location of cylinders there are engines with a vertical or inclined location of cylinders in one row, V-shaped with an arrangement of cylinders at an angle (at an arrangement of cylinders at an angle the 180th engine is called as the engine with opposite cylinders); On a way of cooling - on engines with liquid or air cooling; By the form of applied fuel - petrol, diesel, gas and multifuel; On extent of compression. Depending on compression ratio distinguish engines with high (E = 12... 18) and low (E = 4... 9) compression; on a way of filling of the cylinder with a fresh charge: engines without pressurization at which the admission of air or gas mixture is carried out at the expense of a discharging in the cylinder at a soaking-up piston stroke; engines with pressurization at which the admission of air or gas mixture in the working cylinder occurs under the pressure created by the compressor (this technology is needed for the purpose of increase in a charge and obtaining the increased engine capacity); on frequency of rotation: low-speed, the increased frequency of rotation, high-speed; to destination distinguish engines stationary, autotractor, ship, diesel, aviation (Dyachenko N. H 1974) .

3.2. Bases of the piston ICE

Internal combustion piston engine consists of mechanisms and the systems carrying out specified functions and cooperating among themselves. The main parts of such engine are the crank-type mechanism and the gas-distributing mechanism, and also power supply systems, cooling system, ignitions and lubricant system.

The crank-type mechanism will transform rectilinear reciprocation of the piston to a rotary motion of a cranked shaft.

The mechanism of a gas distribution provides a timely admission of gas mixture in the cylinder and removal of products of combustion from it.

The power supply system is intended for preparation and supply of gas mixture in the cylinder, and also for branch of products of combustion.

The lubricant system serves for supply of oil to cooperating details for the purpose of reduction of force of a friction and their partial cooling, along with it circulation of oil leads to washing off of a deposit and removal of products of wear process.

The system of cooling supports normal temperature power setting, providing objection of heat from details of cylinders of piston group and from the valve mechanism group which are strongly heating up at combustion of a working mix of.

The system of ignition is intended for ignition of a working mix in the engine cylinder.

3.2.1. Working cycle of the ICE

Internal combustion engines in cars are called so, because combustion of fuel occurs directly in the cylinder. There are some main details of ICE, except the cylinder. For, example, the piston, a rod, a crankshaft. On a crank of a crankshaft the rod is movably fixed. The piston is fastened to the rod. The cylinder is closed by a cover which is called as a cylinder head. In a head there is a deepening which is called as combustion chamber. Also there are the inlet and outlet openings closed by valves in a head. The flywheel is fastened to a crankshaft – a massive round disk.

There is a piston moving in the cylinder when rotation of the crankshaft is going on. Extreme top position of the piston is called as the top dead center (T.D.C.), extreme bottom situation – the bottom dead center (B.D.C.). The distance, which passes the piston between dead centers, is called as a piston stroke. The space being over the piston, when it is in B.D.C., is called as working volume of the cylinder. When the piston is in T.D.C., there is a space over it called as a volume of the combustion chamber. The sum of working volume and volume of the combustion chamber is called as full volume of the cylinder. The volume is specified in liters or cubic centimeters in technical data. The volume of the multicylinder engine is equal to the sum of full volumes of all its cylinders. The relation of full volume of the cylinder to volume of the combustion chamber is called as compression ratio of the engine. It shows, in how many time a working mix in the cylinder is compressed (Samsonov V. I. 1990).

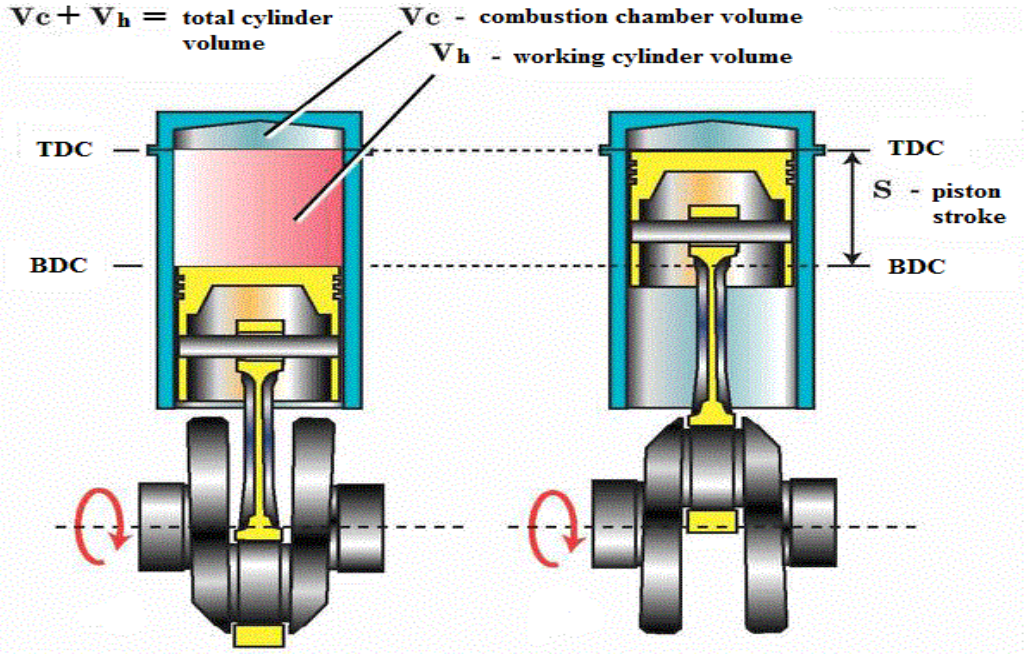

Figure 17. Parameters curve of the connecting-rod gear.

One piston stroke from one dead center to another is called as a step. The crankshaft thus makes a half turn. During the first step there is an admission of gas mixture in the cylinder. The valve of the inlet opening is opened, the valve of the outlet opening is closed. The piston, moving from T.D.C. to B.T.C, like the pump, creates a discharging in the cylinder and the fuel, mixed with air, fills it.

During the second step, at piston movement from T.D.C. to B.T.C, there is a compression of gas mixture. Thus both outlet and inlet valves are closed. As a result pressure and temperature in the

cylinder increase. At the end of a compression step when piston is going closer to the T.D.C., gas mixture is set on the fire by a spark from a spark plug (in petrol ICE) or self-ignites from compression (in diesel ICE).

There is a combustion of the working mix during the third step. The valves remain closed. The ignited working mix sharply increases temperature and pressure in the cylinder which forces the piston to move down with effort. The piston through a rod transfers effort to the crankshaft, creating a torque on it. Thus, there is a transformation of energy of fuel combustion to mechanical energy which moves the car. Therefore this step is called as a driving stroke. The flywheel, fixed on the crankshaft, reserves energy, providing crankshaft rotation with help of the inertia forces during the preparatory steps.

There is a production of exhaust gases and cylinder cleaning during the fourth step. The piston, moving from T.D.C. to B.T.C, pushes out burning products via the open outlet valve.
Further all process repeats. Thus, the working cycle of described ICE consists of four steps. Therefore it also is called as four-cycle. The crankshaft during this time makes two turns. There are also two-stroke engines in which the working cycle occurs for two steps. However, such IC engines on cars practically are not applied now (Orlin A. S. et al. 1983).

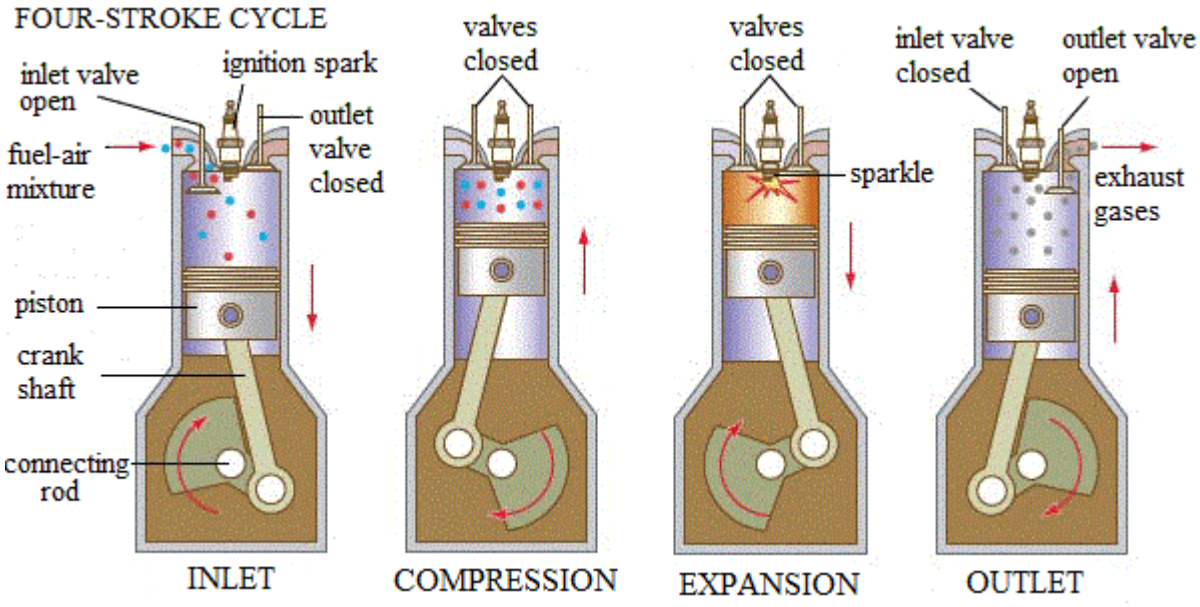

Figure 18. Working cycle.

All steps of a driving stroke in different cylinders should occur in a certain sequence for smooth operation of the multicylinder engine and reduction of non-uniform loadings on the crankshaft.

Such sequence is called as an engine operating procedure. It is defined by an arrangement of necks of the crankshaft and camshaft cams. For example, the operating procedure in VAZ engines is 1-3-4-2. The full cycle in each cylinder in the four-cycle engine is made for two turns of the crankshaft, therefore, there should be the operating stroke in the four-cylinder engine for its uniform work for every half turn of the crankshaft in one of cylinders.

The considered details make in aggregate the crank-type mechanism. Except it, the gas-distributing mechanism, cooling system, greasing system, a power supply system and ignition system (in petrol engines) are also necessary for ensuring work of ICE.

The gas-distributing mechanism, controlling operation of valves, provides their timely opening and closing. The system of cooling takes away heat from the details of the engine which are heating up at work. The lubrication system submits oil to the sliding surfaces. The power supply system serves for preparation of a working mix and its supplying to the cylinders. The ignition system transforms low-voltage tension from accumulator storage battery in high-voltage and submits it on spark plug for ignition of a working mix.

The substance by means of which the valid working cycle of the engine is carried out is called as a working body. Properties of a working body change during the commission of cycle depending on its structure and temperature. The substance, which has arrived in the cylinder by the beginning of process of compression, is called *a fresh charge*. During compression by a working body, *the working mix* occurs, representing a mix of a fresh charge and *residual gases* that are the products of the combustion, which have remained in the cylinder after the previous cycle. During combustion there are chemical reactions at which combustion products are formed of a fresh charge. Thus products of combustion are a working body in expansion and release steps.

Atmospheric air contains 21 % (on volume) or 23 % (on weight) of the oxygen participating in process of combustion (oxidation) of fuel, and 79 % of the inert gases for reaction of combustion of gases (generally - nitrogen).

The amount of air in *kmole* or in *the kg*, which is theoretically necessary for full combustion of 1 *kg* of fuel, depends on elementary composition of fuel.

$$L_o = \frac{1}{0.21}\left(\frac{C}{12} + \frac{H}{4} - \frac{O}{32}\right) \quad (3.1)$$

$$I_o = \frac{1}{0.23}\left(\frac{8C}{3} + 8H - O\right) \quad (3.2)$$

Here: *C*, *N* and *O* – mass fractions of carbon, hydrogen and oxygen in 1 *kg* of fuel (*C* + *N* + *O* = 1).

3.3. Key parameters of working process

For convenience of calculations and comparison of different engines on quantity of the performed work of the cycle and its costs on overcoming of the mechanical losses in the theory of working process use conditional (fictitious, really nonexistent) parameters under the name of the mean indicated pressure p_i, mean pressure of mechanical losses p_M and mean effective pressure p_e.

The physical essence of these parameters is identical – they are specific work of a cycle, i.e. the work which is received or spent for unit of working volume of the cylinder. It follows from this, that:

$$p_i = \frac{L_i}{V_h}, p_M = \frac{L_M}{V_h}, p_e = \frac{L_e}{V_h}, \quad (3.3)$$

where *Li* – indicated (internal) complete work of expansion of gases in the cylinder for a cycle; L_M – the work spent for overcoming of mechanical losses in the engine for a cycle (a friction, a drive of auxiliary mechanisms, implementation of gas exchange processes). It is a part of indicated work of a cycle; *Le* – the effective (valid) work transferred through the crank-type mechanism to the consumer for a cycle. It is a part of indicated work of a cycle.

As mean indicated pressure (or the mean pressure of mechanical losses, the mean effective pressure) is called such conditional (fictitious, really not existing), constant on size, excess pressure in the cylinder which, affecting the piston, completes for one stroke from T.D.C. to B.D.C. the work which is equal to the indicated work of a cycle (or the work spent for overcoming of mechanical losses, or effective work for a cycle).

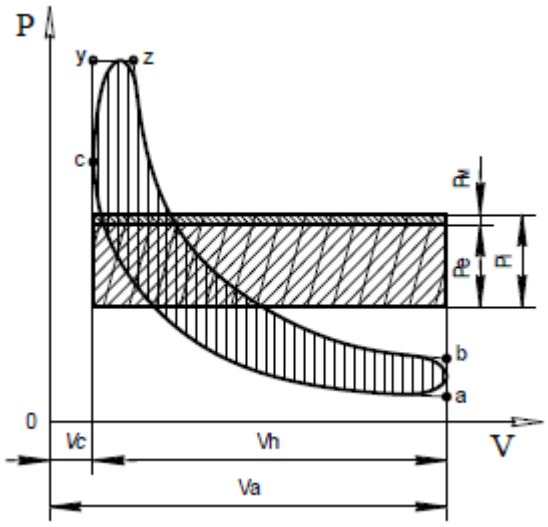

Figure 19. To concept definition of «mean pressure».

Pressurization pressure p_k.

Exact determination of pressurization pressure p_k for various types of diesel engines and systems of pressurization inconveniently as p_k has difficult interrelations with many parameters of working process. At p_k choice we can usually be guided by its value at a prototype, correcting it in the bigger or smaller party depending on a ratio of mean effective pressure at a prototype and the designed engine.

Decrease in temperature of the boost air in an air cooler ΔT_x and its resistibility Δp_x.

In diesel engines with pressurization temperature of the boost air after compression in the centrifugal compressor T'_k reaches 90... 200 ∘ C . It is usually applied cooling of the boost air to increase the efficiency of pressurization. Because of this technology the power raises and thermal stress of a diesel engine goes down.

The power raises because of increasing in density of inflatable air: at bigger density of air the mass of a charge increases, when cylinder is filling, that allows to burn more fuel and, in addition, to increase diesel engine power.

Thermal stress of a diesel engine goes down, when the boost air is cooling because of fall of charge temperature. As a result, level of working body temperature in the cylinder decreases throughout all cycle and, therefore, temperature of details of the sleeve assembly also goes down. Usually, the air cooler is established, when the temperature of the boost air t_k exceeds 55... 60 ℃.

Heating of the air in the cylinder ΔT_a.

The air which has arrived in the cylinder during of filling is warmed up from cylinder walls by the end of process on the size ΔT_a and will have temperature T_k+ΔT_a, where T_k – air temperature in front of the inlet valve (at a diesel engine without T_0 pressurization).

As a result of mix of the air in the cylinder with the residual gases, which have the temperature T_r, the working mix with T_a temperature is formed.

According to skilled data, the heating of air from cylinder walls of four-cycle diesel engines is ΔT_a =5... 20 and the range for duple is a little bit less (ΔT_a =5... 10 T_0).

Residual gases coefficient.

The exhaust gases, which have remained in the cylinder after a step of release in volume of the compression chamber V_c, are called as residual gases.

The relation of amount of residual gases M_r to amount of the air L, which has arrived in the cylinder, is called as residual gases coefficient:

$$\gamma_r = \frac{M_r}{L} \tag{3.4}$$

The coefficient γ_r depends on:

– existence of pressurization and its degree;
– frequencies of rotation;
– compression ratio ε;
– residual gases pressure p_r and temperature T_r;
– difference of pressure between inlet p_k and outlet p_p receivers;
– cylinder sizes;
– design features of gas exchange system and outlet path.

Residual gases temperature T_r

According to skilled data, the residual gases temperature T_r:

Four-cycle diesel engines:

without pressurization 600... 800 K
with pressurization 700... 1000 K

Duple diesel engines 700... 800 K

The residual gases temperature T_r generally depends on:

– air excess coefficient α;
– absence or existence of pressurization and its degree;
– rapidities.

Compression ratio.

Distinguish nominal (geometrical) compression ratio ε and the valid compression ratioε. Nominal compression ratio is the relation of full volume of the cylinder V_a (at the moment when piston is in B.D.C.) to the compression chamber volume V_c.

$$\varepsilon = \frac{V_a}{V_c} = \frac{V_h + V_c}{V_c} = \frac{V_h + 1}{V_c}, \tag{3.5}$$

where compression chamber volume:

$$V_c = \frac{V_h}{\varepsilon - 1} \tag{3.6}$$

Working cylinder volume:

$$V_h = V_c(\varepsilon - 1) \tag{3.7}$$

The valid compression ratio ε_d represents the relation of cylinder volume at the moment of closing of bodies of a gas distribution ($V_c + V_h - \Psi V_h$) to the compression chamber volume V_c:

$$\varepsilon_d = \frac{V_c+V_h-\Psi V_h}{V_c} = 1 + \frac{V_h}{V_c}(1 - \Psi), \quad (3.8)$$

where Ψ – a share of a piston stroke S on the compression step, taken with gas exchange processes. It corresponds to cylinder volume from B.D.C. till closing of outlet valves in four-cycle engines and closings of blowing-off or exhaust windows in two-stroke engines.

Air excess coefficient.

The relation of the air valid quantity participating in process of combustion to theoretically necessary is called as air excess coefficient for combustion.

Kmole is a substance unit of quantity, fundamental unit in the international system of units (SI). Kmole of any gas is amount of the gas which weight is equal in kgs to molecular mass of this gas.

$$\alpha = \frac{L}{L_0} \quad (3.9)$$

where L and L_0 the valid and theoretically necessary amount of the air participating in combustion respectively.

Pressure increase ratio λ and maximum combustion pressure p_z.

Pressure increase ratio during combustion λ is understood as the relation of the maximum combustion pressure p_z to pressure at the end of compression p_c.

$$\lambda = \frac{p_z}{p_c} \quad (3.10)$$

At calculations of working processes value of the pressure p_z usually is accepted on the basis of skilled data of prototypes of the designed engine or is defined from expression $p_{z=} \lambda p_c$ after a preliminary choice of pressure increase ratio λ.

Extraction coefficient χ and heat-availability factor ξ.

Indicator of quantity of the heat which is extracting during combustion of the fuel is heat extraction coefficient. Heat extraction coefficient represents a share of lower heating value Q_{LHV} of the fuel, extracted to the considered moment of working process taking into account heat losses on incompleteness of combustion Q_{ic} and dissociation *Qdis*.

$$\chi = \frac{(Q_{LHV} - (Q_{ic} + Q_{dis}))}{Q_{LHV}} \tag{3.11}$$

In calculations, there is lower heating value of the fuel, which less than the highest (physical) on figure of heat of vaporization of the water which is forming during combustion of hydrogen of the fuel. As the temperature of exhaust gases is much higher than temperature of condensation of water vapor, heat of vaporization does not come back to a cycle and is not used for receiving work.

Share of lower heating value of the fuel, which is used for increase of internal energy of a working body and commission of external mechanical work on combustion and expansion lines with the additional accounting of losses in cooled water Q_{ω}, i.e. all losses of heat, is estimated by heat-availability factor ξ.

$$\xi = \frac{(Q_{LHV} - (Q_{ic} + Q_{dis} + Q_{\omega}))}{Q_{LHV}} = \chi - \frac{Q_{\omega}}{Q_{LHV}} \tag{3.12}$$

Factors ξ and χ are thermal emission characteristics during combustion in the real engine and are defined by practical consideration.

3.4. Determination of gas exchange parameters

Air pressure at the compressor outlet p'_k.

$$p'_k = p_k + \Delta p_x \tag{3.13}$$

where p_k – pressurization pressure, *MPa*; Δp_x – air cooler resistance, *MPa*.

Air temperature at the compressor outlet T'$_k$.

As a result of polytropical compression of the air in the compressor we will receive:

$$T'_k = T_0\left(\frac{p'_k}{p_0}\right)^{\frac{n_k-1}{n_k}} \quad (3.14)$$

where n_k is a polytropic index of air compression can be chosen depending on type of the compressor and cooling degree of its frame.

Air temperature in a boost receiver (in front of the inlet valve) T_k.

$$T_k = T'_k - \Delta T_x \quad (3.15)$$

Air temperature in the cylinder at the end of filling T"$_k$ (air is conditionally considered as a separate component of a working mix). A working mix can be considered as mix of air and residual gases in the cylinder.

$$T''_k = T_k + \Delta T_a, \quad (3.16)$$

where ΔT_a is an air heating from cylinder walls.

Residual gases pressure in the cylinder p_r.

$$p_r = (0{,}95 \ldots 1{,}15)\frac{p_k}{p_k/p_p} \quad (3.17)$$

It is also possible to use an experimental ratio

p_r = (0,75... 1,0) p_k, MPa.

Pressure of a charge (a working mix) at the end of filling.

p_a = (0,85... 1,1) p_k, MPa.

Residual gases coefficient.

$$\gamma_r = \frac{T''_k}{T_r}\frac{p_r}{\varepsilon p_a - p_r} \tag{3.18}$$

Charge temperature (a working mix) in the cylinder at the end of filling T_a.

$$T_a = \frac{T''_k + \gamma_r T_r}{1+\gamma_r} \tag{3.19}$$

Coefficient of fullness.

$$\eta_v = \frac{\varepsilon}{\varepsilon - 1}\frac{p_a}{p_k}\frac{T_k}{T_a}\frac{1}{1+\gamma_r} \tag{3.20}$$

The relation of amount of the air which has really arrived in the cylinder G_d to that amount of air G_h which could take place in working volume of the cylinder V_h at temperature and pressure in front of inlet valves (T_k and p_k at diesel engines with pressurization, T_0 and p_0 at diesel engines without pressurization) is called as coefficient of fullness η_v.

$$\eta_v = \frac{V_d}{V_h} = \frac{G_d}{G_h} = \frac{G_d}{V_h \rho_a}, \tag{3.21}$$

where ρ_a – air density in front of inlet valves, kg/m3.

3.4.1. Compression process

Compression process in a cycle is intended for increase of pressure and charge temperature in the cylinder for the purpose of ensuring reliable spontaneous ignition and effective combustion of injected fuel on all operation modes, and also for increase in difference of temperatures in a cycle for the purpose of increase of its efficiency. Compression represents the difficult thermodynamic process which is generally determined by the variable intensity and the direction of heat exchange between the arrived air and cylinder walls.

The valid process of compression occurs on a polytrope with an indicator n_1, which is variable on all piston stroke.

The greatest influence on value of the indicator n_1 render:

– turns;
– cylinder sizes;
– absence or existence of pressurization and its degree;
– compression ratio;
– intensity of cylinder cooling.

At the beginning of compression, due to higher surface temperature of the cylinder and the piston with a head in comparison with temperature of a fresh working body, the heat supply from hot surfaces of these elements to a working body takes place.

In process of piston moving to T.D.C intensity of a heat supply from hot walls to the working body falls. At some moment of the process thermal balance is established: the heat supply to the working body is equal to branch of heat from the working body in walls. This moment is called as the moment of the quasi-adiabatic balance.

At further moving of the piston to T.D.C. the temperature of a working body becomes above average temperature of walls (*Tw*). The thermal stream changes the direction. There is a heat return in walls. Due to a big difference of temperatures in the second half of process of compression, especially in diesel engines, heat return in walls prevails over process of a heat supply.

A thermal capacity of a working body in ICE cycle.

The thermal capacity of a physical body is one of its thermodynamic properties and represents the relation of quantity of heat Q, reported to a body, to corresponding change of temperature T of this body.

In real thermodynamic processes a thermal capacity change also depends on temperature, structure of a working body and other factors. Therefore distinguish a true thermal capacity, i.e. at present time of course of process and a conditional mean thermal capacity, a constant in any interval of change of parameters of a working body.

The mean thermal capacity in the range from zero to this temperature T is understood as such conditional constant thermal capacity which work on an increment of temperature gives the same quantity of heat what turns out as a result of integration on variable value of a true thermal capacity.

3.4.2. Combustion process

In the course of combustion the hidden chemical energy of fuel turns into thermal energy of a working body.

The main requirements to process of combustion can be formulated by three provisions:

– the most complete combustion of fuel;
– the best use of oxygen of air;
– optimum course of combustion in time.

These requirements are caused by aspiration to receive high efficiency (small specific fuel consumption) and big specific engine capacity.

The purpose of combustion process calculation is determination of its final parameters – the maximum values of combustion pressure p_z and combustion temperature T_z.

Fuel combustion is the main process of a settlement cycle at which there is an allocation of the heat which is transformed in the engine to useful mechanical work. Spontaneous ignition and combustion represents difficult process of a chemical compound of combustible elements of fuel with the air oxygen, accompanied by heat allocation. At calculation of combustion with help of Grinivetskiy-Mazing method intermediate physical and chemical changes of a working body do not consider and consider only end results of chemical reactions.

Combustion process is counted proceeding from burning of 1 kg of fuel. For convenience of calculations the amount of air and being formed gaseous combustion products measure in kmole. Combustion process calculation consists of two stages. In the first, which is called «the thermochemistry of combustion process», proceeding from stoichiometric ratios (from the combustion reactions equations of fuel components), we define:

– theoretically necessary L_o and valid L;
– amount of air for combustion;
– quantity and structure of combustion products;
– mean isochoric and isobaric thermal capacity of air and combustion products.

The second stage is called «thermodynamics of combustion process». Here, taking into account earlier chosen basic skilled data and settlement results of the first stage, we need to define:

–pressure increase ratio λ;
–preliminary expansion ratio ρ;
– maximum combustion temperature T_z.

Pressure increase ratio λ.

$$\lambda = \frac{p_z}{p_c} \tag{3.22}$$

Pressure increase ratio is one of characteristics of dynamism ("rigidity") of combustion. It depends on rapidity, absence or existence of pressurization and its degree, carburation type. High λ values are characteristic for high-speed diesel engines with a volume atomization of fuel. Application of pressurization causes λ reduction owing to reduction of the delay period duration of spontaneous ignition because of higher temperature in the cylinder at the end of compression at pressurization. High λ values are not peculiar to the divided combustion chambers.

The maximum temperature of gases at the end of visible combustion T_z.

The maximum combustion temperature T_z is defined as a result of the solution of the combustion equation.

The combustion equation is deduced on the basis of the equation transformation of the first law of the thermodynamics which has been written down for a cycle with the displaced heat supply.

Preliminary expansion ratio ρ.

The relation of the cylinder volume at the end of visible combustion V_z to cylinder volume at the end of compression V_c is called as extent of preliminary expansion.

3.4.3. Expansion process

Expansion process is polytropic with the polytrope indicator changing in quite wide limits. Here, unlike compression process, there is a heat return of gases to cylinder walls during all process as the gases temperature is higher than walls temperature.

For simplification of calculation we can accept expansion process passing with a constant mean polytrope value. It accepts in such way that the expansion curve, constructed on the polytrope law, closer approached to the valid expansion process in the cylinder.

With increase in number of turns the indicator n_2 decreases as time of heat exchange of gas with walls is reduced, gas admissions with piston rings decrease. Besides, the torching of fuel, which is not burned in full extent, spreads on the most part of a site of the expansion line; heat, which was allocated, doesn't only compensate heat transfer to walls, but also maintains gas mix temperature approximately a constant.

With loading reduction (at invariable number of turns) the indicator falls as the relative quantity of combustion products and therefore also relative heat transfer to walls decrease.

With increase in the cylinder sizes the polytrope indicator value falls as the relative cooling surface decreases.

The purpose of expansion process calculation is determination of working body parameters in the cylinder at the end of expansion – temperature T_b and pressure p_b.

Subsequent expansion ratio δ.

The relation of the cylinder volume at the end of the expansion V_b to cylinder volume at the end of visible combustion V_z is called as subsequent expansion ratio δ:

$$\delta = \frac{V_b}{V_z} \tag{3.23}$$

Expansion polytrope indicator and temperature at the end of the expansion T_b.

Expansion process proceeds in difficult conditions. It is influenced by a number of interconnected variable factors: pressure and temperature change, heat exchange of gases with walls, torching of fuels in the first part of the process, sometimes being stretched on all process, leakage of gases through thinnesses of piston rings and valves, partial restoration of products of the dissociation, accompanied by allocation of heat, etc. As a result of influence of the listed factors expansion process in the valid cycle occurs on a polytrope which indicator changes on all extent of process.

Mean value of the expansion polytrope indicator n_2:

$$n_2 - 1 = \frac{8{,}314\left(\beta_z \cdot T_z / \beta - T_b\right)}{\frac{Q_H\left(\xi_b - \xi_z\right)}{L(1+\gamma_r)\beta} + \frac{\beta_z}{\beta}\left(a_{v_z} + b_{v_z} \cdot T_z\right)T_z - \left(a_{v_b} + b_{v_b} T_b\right)T_b}. \tag{3.24}$$

Pressure at the end of the expansion p_b.

As a result of transformation of the expansion polytrope equation, pressure at the end of the expansion will be:

$$p_b = \frac{p_z}{\delta^{n_2}} \tag{3.25}$$

3.5. External thermal balance

Distribution of the heat, which is allocating at fuel combustion in the Q_h engine, on useful used heat and different types of thermal losses is called as external thermal balance. Useful heat Q_e is spent for receiving effective work, and thermal losses develop of losses with the cooling environment Q_{cool}, the fulfilled gases Q_{ful} and the unrecorded losses estimated by the residual member of thermal balance Q_{imb} (it is imbalance). The equation of external thermal balance in an absolute form looks like:

$$Q_h = Q_e + Q_{cool} + Q_{ful} + Q_{imb} \quad (3.26)$$

In a relative form the equation has a similar appearance:

$$q_h = q_e + q_{cool} + q_{ful} + q_{imb} \quad (3.27)$$

Distinguish internal thermal balance of the engine in which heat redistribution in the engine between components of external thermal balance is considered and total values of its components are defined.

The external thermal balance usually is defined experimentally. Values of its components allow to judge perfection of heat use and to plan ways of improvement of engine indicators. At design of the new engine for the purpose of receiving basic data for calculation of different systems such as cooling, greasing, determination of thermal losses utilization possibility, external thermal balance is determined by a settlement way.

Quantity of the heat lost in cooling system through its components is possible to calculate on expression:

$$Q_{cool} = Q_{c-e} + Q_{com} - Q_{fil} + Q_{rel} + Q_{tur} + Q_{p-c} + Q_{wp} \quad (3.28)$$

where $Q_{c\text{-}e}$ – heat loss in combustion and expansion process; Q_{com} – heat loss in compression process; Q_{fil} – the heat reported to a fresh charge from walls of the cylinder, i.e. finally from cooling system, in the course of filling (heating of a charge); Q_{rel} – heat loss in cooling system at release; Q_{tur} – heat loss from the turbine (in case of the cooled case); $Q_{p\text{-}c}$ – heat loss to equivalent work of a friction between the piston and the cylinder; Q_{wp} – heat loss to equivalent operation of water pumps. (Operation of water pumps belongs to losses in cooling system because turns into the heat reported to water).

Heat loss with the fulfilled gases.

The heat, which is carried away by final gases, is defined as a difference of gases enthalpy (heat contents) on an exit from the gas turbine and air arriving in the compressor. With air heat from

environment, which is not considered in the heat balance of fuel, is added and should be excluded from it.

$$Q_{ful} = M_g C_{p_{tur}} T_{tur} - M_a C_{p_a} T_0, \quad (3.29)$$

where M_g – an hour consumption of the fulfilled gases, kmole / h; M_a – an hour consumption of air, kmole / h; $C_{p_{tur}}$ and C_{p_a} – a thermal capacity of gases behind the turbine and air, kmole / h; T_{tur} *and* T_0 – temperature of gases behind the turbine and air.

The residual member of thermal balance (it is imbalance) is defined as a difference between the heat, brought with fuel, and the sum of known other components of thermal balance. The residual member considers heat losses from incompleteness of combustion, engine emission in environment and other insignificant losses.

Some parts of thermal balance, received by a settlement way, will be coordinated satisfactory with experimental data and can be used for design of auxiliary systems and engine units.

In structure of heat losses in cooling system the greatest value is made by losses in the process of combustion – expansions. Losses at release, from a friction in pair piston – the cylinder, at compression, on a drive of water pumps and a heat supply in the course of filling owing to heating of a charge have a little bit lower values (Vasiljev V. A. 1987).

4. HEAT FLUX MEASUREMENT TECHNIQUES INSIDE INTERNAL COMBUSTION ENGINE

In modern internal combustion engines (ICE) we strive to force working process that increases thermal loads on details of sleeve assembly. The heat flux density reaches 10^6 W/m^2 and more, it considerably changes during a cycle and is non-uniform on surfaces of heat exchange.

For an assessment of a thermal condition of ICE's details it is necessary to have not only mean density values on a surface, but also local values of heat flux density as functions of the crank angle of a cranked shaft (Kavtaradze R. Z. 2001).

Until present time direct (with aid of the Heat Flux Sensors) receiving local heat flux density on the surfaces, limiting gas volume or a working mix in the cylinder, was not carried out. At the same time interest of researchers to the measurement of heat flux grows in these conditions, and they determine a heat flux by a "semi-settlement" method. In the beginning thermometry is conducted with aid of quick-response thermocouples, and then we use one of the solutions of the heat conduction problem, priori specifying boundary conditions.

Let's consider one work (Chang, J. et al. 2005) devoted to the heat flux definition on the bottom of the piston in the petrol engine with Homogeneous Charge Compression Ignition (HCCI). As the measuring converter serves coaxial (diameter of 1,52 mm) the iron-constantan thermocouple; the worker juncture is created by a foil in thickness 1 … 2 microns that provides a constant of time about 10-6. The estimated error of the thermometry, according to the authors, do not exceed 2 %. One group of thermocouples took temperature on the piston bottom, another was closed up on depth of δ =4 mm to estimate a stationary component of the heat flux density.

The surface temperature was defined as:

$$T(\tau) = T_m + \sum_{n=1}^{N} A_n \cos(n\omega\tau) + B_n \sin(n\omega\tau), \qquad (4.1)$$

and the heat flux density on a surface was summarized from stationary and dynamic components:

$$q = \frac{\lambda}{\delta}(T_m - T_l) + \lambda \sum_{n=1}^{N} \Phi_n \left[(A_n + B_n)\cos(n\omega\tau) - (A_n - B_n)\sin(n\omega\tau) \right]; \quad (4.2)$$

here *Tm*, *Tl* – average temperatures on depth δ and on the bottom of the piston, respectively;

τ – current time;

λ – thermal conductivity of the piston material;

An, *Bn* – the amplitude functions defined by fast transformation of Fourier;

ω – rotation frequency of the cranked shaft;

N–number of members of the row which is needed to be summarize;

n– the current number of members of the row.

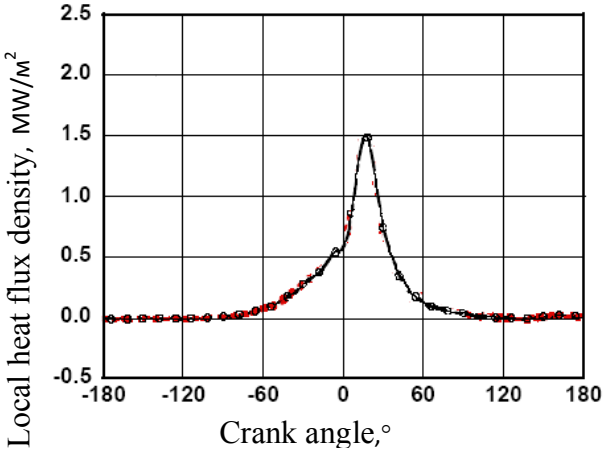

Figure 20. Dependence of local heat flux density from the crank angle(Chang, J. et al. 2005).

As a result at *N* = 40 (authors consider that is enough to use this number of members for permission in 0,5° of crank angles of a cranked shaft) dependence *of q* (φ), presented on figure 20, is received. Maximum shift to the right from the top dead center is clearly visible. This fact, in our opinion, is physically disputable – or, at least, demands detailed justification.

On an example of this carefully performed and honestly described work we see that the "semi-settlement" approach has been practically exhausted, and researchers have even no aspiration to a direct measurement of heat flux – that apologizes, of course, absence of heat flux sensors with demanded (and very high) characteristics.

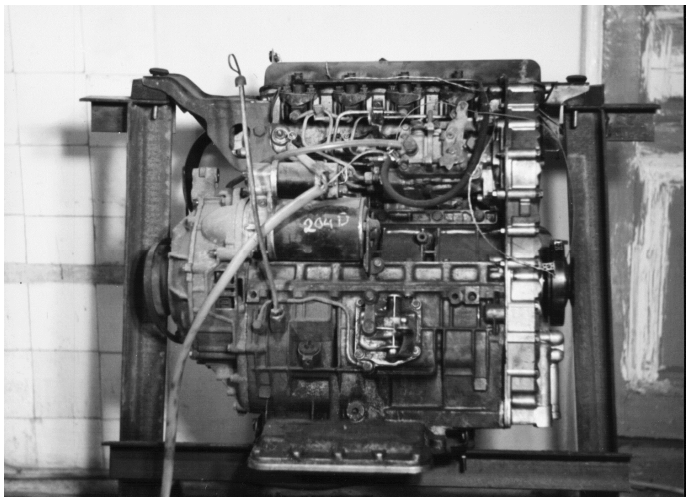

Figure 21. A general view of the Indenor 4Ch7,8/7,1 engine at the stand

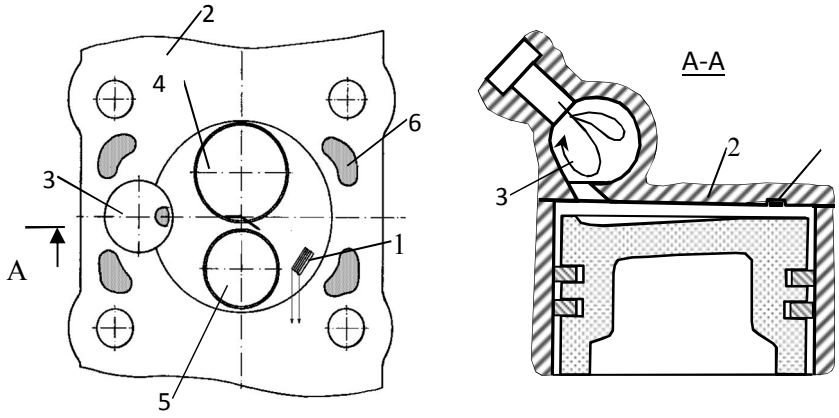

Figure 22. GHFS installation site on the surface of the cylinder cover:
1–GDTP; 2– the cylinder cover; 3–vortical chamber; 4–inlet valve; 5–outlet valve; 6– channels of the cooling system.

Application of GHFS allowed to investigate non-stationary heat transfer from gas to a surface of the combustion chamber of the four-cycle diesel Indenor XL4D engine. The manufacture of this engine is PCA Peugeot Citroën concern and it was provided by Menovehje AY firm (Finland). There are some main characteristics of the engine: turbulence-chamber, compression ratio of 23, the maximum capacity of 35 kW at 5000 rpm, the maximum torque of 84,3 Nanometers ·at 2500 rpm.

All experiments was a pilot version, the preparation of the engine elements was minimized. In these conditions GHFS was placed on a fire surface of the combustion chamber to run the wires in the most convenient way. Essentially, it is clear, that it is possible to measure, by a similar

way, local values of the heat flux density in other zones of a fire surface where mean temperature for a cycle does not exceed limits of thermal stability of GHFS on the basis of bismuth.

The engine fixed on a frame (figure 21), was connected to power supply systems, start, cooling, production of exhaust gases, measurement and registration of signals. The installation site of GDTP and design features of installation are shown on figures 22 and 23.

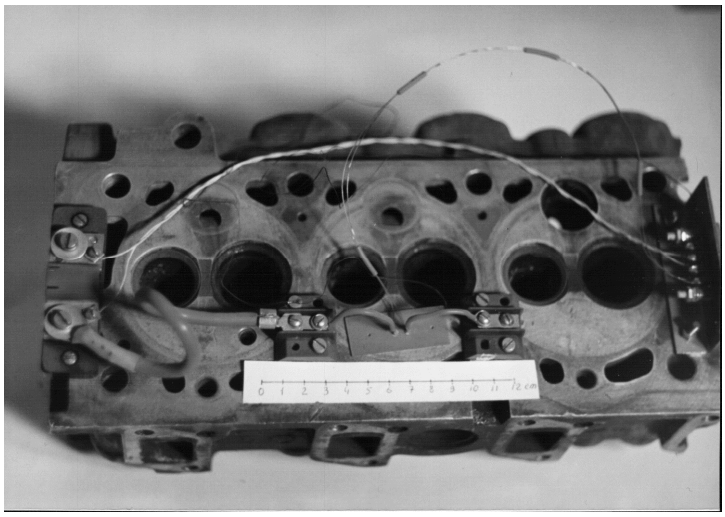

Figure 23. A general view of the cylinder cover with established GDTP
(before calibration)

GHFS was applied for measurement of local heat flux density on a fire surface of the cylinder cover 2 (figure 22).

Thermal electromotive force of the sensor was measured by light-beam oscillograph N-145. Besides, time marks (50 Hz) and marks of the top dead center (TDC) were registered on the oscillograph chart for the studied cylinder. After GHFS was established on the cylinder cover (Figure 23), there was conducted a calibration of the device by specially developed technique.

In the first series of the experiments a cranked shaft scrolled without supply of fuel (on frequencies of 250 and 870 rpm), in the second, fuel moved according to the regular scheme, and frequencies made of 900 and 1320 rpm. Oscillograph chart, on which change of local heat flux density is presented, are presented on figure 24.

It is visible that the heat flux density in TDC is a maximum. As appears from the thermodynamic analysis of the ICE cycle, the most profitable way is to burn fuel as close to TDC as it is possible (Orlin A. S. et al. 1971). However, dependences of a heat flux on a crank angle of a cranked shaft, on which maximum of heat flux density "lags behind" from TDC, are given in all works on a measurement of heat flux in ICE (Wimmer A. et al. 1999). It is caused, in our opinion, by a big time constant of the traditionally applied thermoreceivers, and also that change of walls temperature of the combustion chamber (and, therefore, thermocouples) usually lags behind change of gas temperature that brings a phase mistake in the heat flux which is calculated according to thermometry.

In our experiments distinction in amplitude of fluctuations of a heat flux in other cycles (Figure 24, a – d) was also observed, on what other experimentators also paid attention. It can be caused both unevenness in movement of a charge, and unevenness in fuel supply from a cycle to a cycle.

There is a reduction of the heat flux density on a curve at the moment of opening of the outlet valve (Figure 24, a,b).

At the engine motoring run without fuel supply (Figure 24, a,b) the density of the local heat flux accrues from zero, reaches a maximum in TDC, and then decreases.

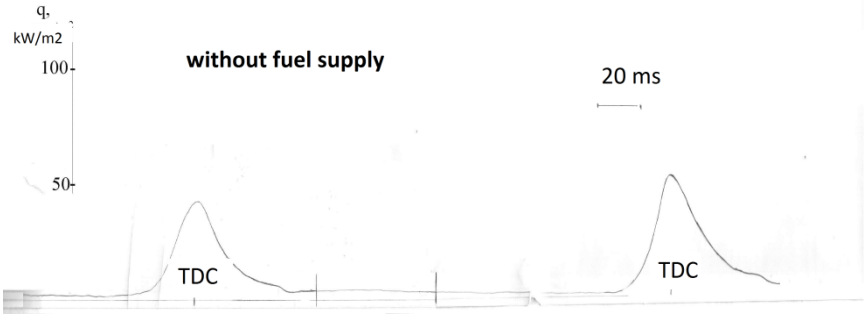

a)

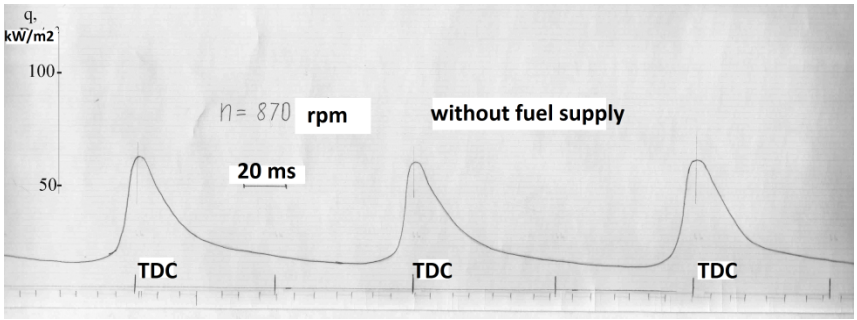

b)

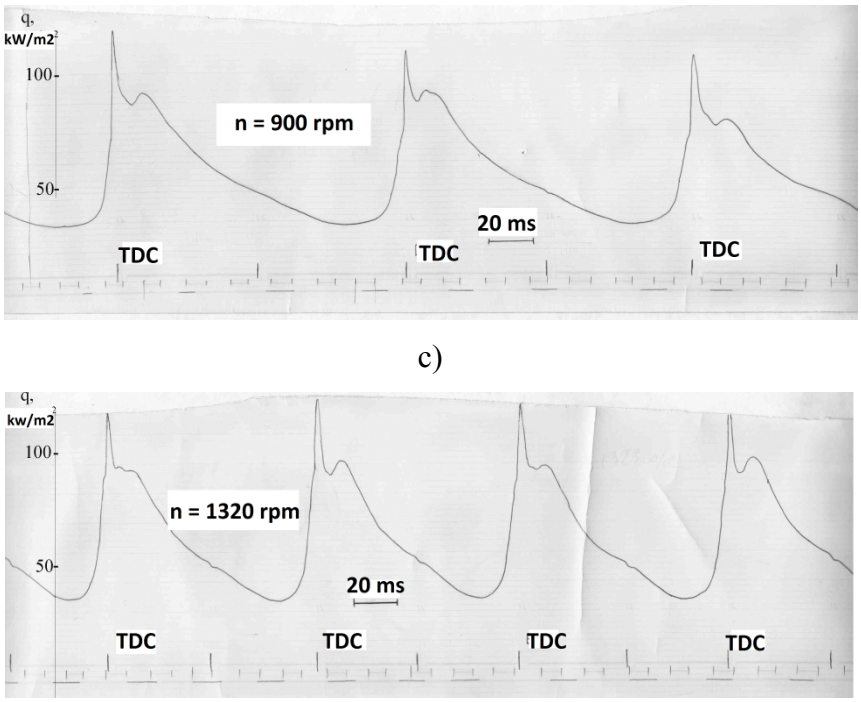

Figure 24. Oscillograph chart of the local heat flux density on a fire surface of the combustion chamber: a – without fuel supply, 250 rpm;
b – without fuel supply, 870 rpm; c – combustion, 900 rpm;
d – combustion, 1320 rpm

At fuel combustion (Figure 24, c, d) there are two maximum of the heat flux that is characteristic for engines with the divided combustion chambers. The first maximum is reached near TDC, and the second – in 70 °... 80 ° from TDC. The theory and physical ideas of such process are reported in special literature (Kostin A. K. 1989),however, «the double maximum» had no experimental confirmation before these experiments – first of all, because of the absence of high-speed heat flux sensors.

On the oscillograph chart the moments of opening of the outlet valve and fuel injection are visible also. In a point of overlapping of valves (near TDC) the heat flux density changes approximately on 2 kW/sq.m. This fact can be connected with heat exchange at a cylinder purge. Figure 25 is constructed as a result of processing of oscillograph chart and let us see a picture more clearly.

It is interesting that on all curves the heat flux keeps a sign. It testifies that the fire surface in a zone of measurement does not manage to be cooled in an absorption step, and the heat flux only pulses. On other sites of the combustion chamber and the cylinder it is possible also sign-variable (on a heat flux) mode.

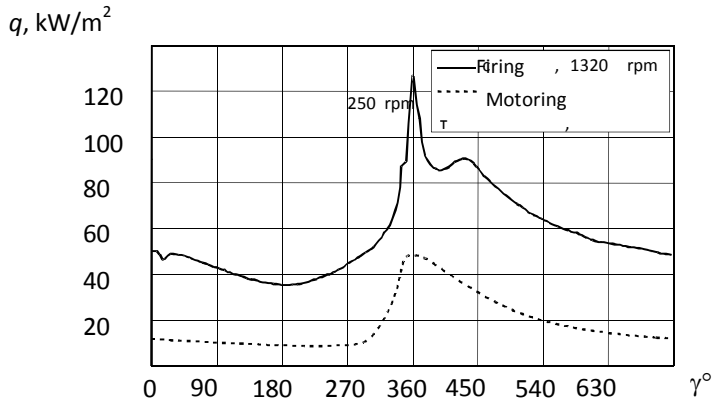

Figure 25. Dependence of the local heat flux density
from the crank angle of the cranked shaft.

The range of the GHFS time constant, which was established before (10–8 … 10–9 c), does them suitable for a measurement of heat flux in engines practically for any rapidity, but the temperature restrictions, mentioned at the beginning of the section, unfortunately, are insuperable. Therefore, it is reasonable in the beginning to carry out thermometry, to define modes, in which the wall temperature does not exceed the level which is admissible for sensors, and then we need to establish GHFS instead of thermocouples. In the long term it is necessary to create more heat-resistant GHFS; only in this case, researches of the heat fluxes on the fire surfaces of the ICE become rather informative.

5. SINGLE-ZONE THERMODYNAMIC MODEL OF AN INTERNAL COMBUSTION ENGINE

In this chapter I would like to give a description of engine simulation model, developed by Kyung Tae Yun et al. This model helps us to compare numerical results, obtained with aid of engine simulation model, and data which we get from experiment, mentioned above.

I would like to introduce a single-zone thermodynamic model of an internal combustion engine. The thermodynamic model is developed on base of the engine model which was described in different papers, for example, in the work was written by Yusaf andYusoff (Yusaf T. F. et al. 2005). We are interested to obtain such parameters as temperature (T), pressure (P), and mass trapped (m) in the cylinder for a full cycle of the crank angle (h). Let's apply the first law of thermodynamics for an open system to an engine cylinder (Kyung Tae Yun et al. 2012):

$$\frac{dU}{d\theta} = \frac{dQ}{d\theta} - \frac{dW}{d\theta} + \sum_i^n \frac{dH_i}{d\theta} \tag{5.1}$$

i – refers to inlet or outlet for the open system;
Q – net heat into the cylinder;
Q_c - heat release during the combustion process;
Q_{ht} - heat transfer through the cylinder walls.

Assume that we have an ideal gas. We can rewrite the equation in terms of the cylinder temperature (T):

$$m \cdot C_v \cdot \frac{dT}{d\theta} + u \cdot \frac{dm}{d\theta} = \frac{dQ_c}{d\theta} - \frac{dQ_{ht}}{d\theta} - \frac{m \cdot R \cdot T}{V} \cdot \frac{dV}{d\theta} + \sum_i (h_i \cdot \frac{dm_i}{d\theta}), \tag{5.2}$$

m - the gas mass in the cylinder;
c_v - the specific heat at constant volume ;
R - gas constant;
V - cylinder volume;
h – enthalpy.

Engine geometry.

We can write the equation for cylinder volume:

$$V = \frac{V_d}{r-1} + \frac{V_d}{s_c} \cdot (\frac{s_c}{2} + l_c - [(l_c^2 - (\frac{s_c}{2})^2 \cdot \sin^2(\theta))^{0.5} + \frac{s_c}{2} \cdot \cos(\theta)], \quad (5.3)$$

V_d - the displacement volume;

r - the compression ratio;

s_c - the stroke;

l_c - the length of the connecting rod.

Net heat release.

The chemical heat release rate can be expressed by:

$$\frac{dQ_c}{d\theta} = Q_t \cdot \frac{dx_b}{d\theta}, \quad (5.4)$$

where Q_t is the total chemical energy released during the combustion process and it can be calculated by:

$$Q_t = m_{fuel} \cdot Q_{LHV}, \quad (5.5)$$

m_{fuel} - the cylinder mass content during one engine cycle;

Q_{LHV} - lower heating value of fuel.

To express X_b (the mass burned fraction) we need to use the Wiebe function:

$$x_b = 1 - \exp[-a \cdot (\frac{\theta - \theta_c}{\theta_d})^{n_w+1}], \quad (5.6)$$

a and n_w - Wiebe function parameters;

θ_c - the crank angle at the start of combustion;

θ_c - duration of combustion process measured in degrees of crank angle.

Net heat transfer.

The rate of heat transfer between the in-cylinder gas mixture and the cylinder walls is evaluated as follows (Kyung Tae Yun et al. 2012):

$$\frac{dQ_{ht}}{d\theta} = \frac{h \cdot A_w \cdot (T - T_w)}{2 \cdot \pi \cdot N_e}, \tag{5.7}$$

T - the mean gas temperature in the cylinder, K;
T_w - the cylinder wall temperature, K;
A_w – surface;
h_t - the heat transfer coefficient.

h_t can be expressed using the Woschni heat transfer correlation:

$$h_t = 3.26 \cdot P^{0.8} \cdot w^{0.8} \cdot B^{-0.2} \cdot T^{-0.55}, \tag{5.8}$$

b - the cylinder bore;
w - the average in-cylinder gas velocity during combustion, m/s:

$$w = C_1 \cdot (2 \cdot N_e \cdot s_c) + C_2 \cdot \frac{V_d \cdot T_o}{P_o \cdot V_o} \cdot (P - P_m), \tag{5.9}$$

where V_d is the piston displacement, C_1 = 2.28 and C_2 = 0.0034 are model constants during the combustion and expansion stroke. However, during the intake, compression and exhaust strokes the average gas velocity is assumed to be proportional to the mean piston speed.

Gas property relationships.

Zucrow and Hoffman's equation (Yuh – Yih Wu, 2006) is used to calculate the ratio of specific heats γ for the air and fuel mixture as a function of temperature. To simplify this equation we can use a quadratic interpolation:

$$\gamma(T) = 1.458 - 1.628 \cdot 10^{-4} \cdot T + 4.139 \cdot 10^{-8} \cdot T^2, \tag{5.10}$$

where T – the cylinder temperature, K. The following equation is needed to express the specific heat at constant volume:

$$c_v(T) = \frac{R}{\gamma(T) - 1}, \tag{5.11}$$

And, finally, write the equations for the specific internal energy and enthalpy:

$$u(T) = \int \frac{R}{\gamma(T) - 1} dT, \tag{5.12}$$

$$h(T) = \int \frac{R \cdot \gamma(T)}{\gamma(T) - 1} dT\,. \tag{5.13}$$

Gas exchange process.

To express the intake and exhaust gas exchange process we need to use the equations for gas flow through a nozzle. The following equation is for calculation of the mass flow rate (Heywood J. B. 1998):

$$\frac{dm}{d\theta} = \frac{C_D \cdot A_v \cdot P_s}{N_e \cdot \sqrt{RT_s}} \cdot \left(\frac{P_v}{P_s}\right)^{1/\gamma} \cdot \sqrt{\frac{2 \cdot \gamma}{\gamma - 1} \cdot \left[1 - \left(\frac{P_v}{P_s}\right)^{\frac{\gamma - 1}{\gamma}}\right]}, \tag{5.14}$$

For a choked flow:

$$\frac{dm}{d\theta} = \frac{C_D \cdot A_v \cdot P_s}{N_e \cdot \sqrt{RT_s}\,\gamma^{1/2} \cdot \left[1 - \left(\frac{2}{\gamma + 1}\right)^{\frac{\gamma + 1}{2 \cdot (\lambda - 1)}}\right]}, \tag{5.15}$$

$$A_v = \frac{\pi \cdot D_v^2}{4}, \tag{5.16}$$

the subscript *s* refers to the stagnation condition;
the subscript *v* – to the valve condition;

C_D - the valve discharge coefficient;

A_v - the reference valve area.

Is we assume that trapped gas behaves like ideal gas, the cylinder pressure is expressed in terms of volume, temperature and mass in the cylinder.

A flowchart that summarizes the proposed engine model is presented in figure 26.

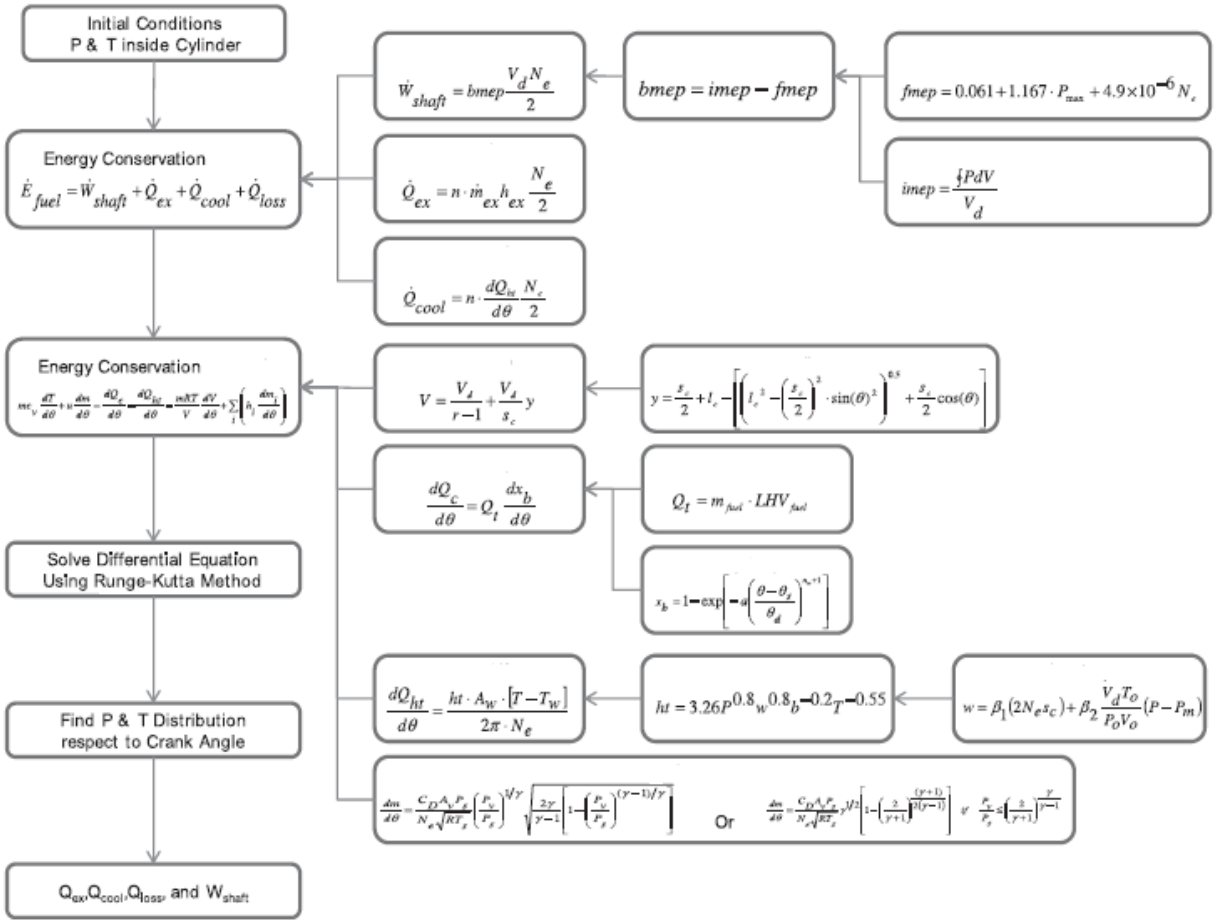

Figure 26. Flow chart of IC engine modeling process.

6. EXPERIMENTAL RESULTS IN COMPARISON WITH MODELING DATA

Numerical results of engine simulation were obtained for the engine speed 1320 rpm (22 rev/s). To evaluate the heat flux, the wall temperature is needed. Since T_w varies considerably with the crank angle, engine speed and load, it is difficult to numerically simulate the detailed wall temperature profile. In paper (Hauser R. L. 1985), an empiric formula was utilized to evaluate the variation of T_w with crank angle:

$$T_w = 1408.7 - 9.3021 \cdot N_e + 4.7205 \cdot 10^{-3} \cdot N_e^2 - 2640.1 \cdot P_m + 1423.4 \cdot P_m^2 + 9.8922 \cdot N_e \cdot P_m, \quad (6.1)$$

Table 3. Estimated engine parameters used in the simulation model.

Parameter	Value
Initial pressure (P_o)	101.325 kPa
Initial temperature (T_o)	298 K
Initial mass (m_o)	0.35 g
Low Heating Value of fuel	45000 kJ/kg
Start of combustion (θs)	50 deg BTDC
Burn duration (θd)	50 deg BTDC
Intake valve diameter (D_{iv})	0.25×B
Exhaust valve diameter (D_{ev})	0.15×B
Maximum valve lift (L_v)	0.1×B
Wiebe efficiency factor (a)	5
Wiebe form factor (n_w)	2

Figure 27 shows the gas temperature variation over the engine cycle according to the proposed model.

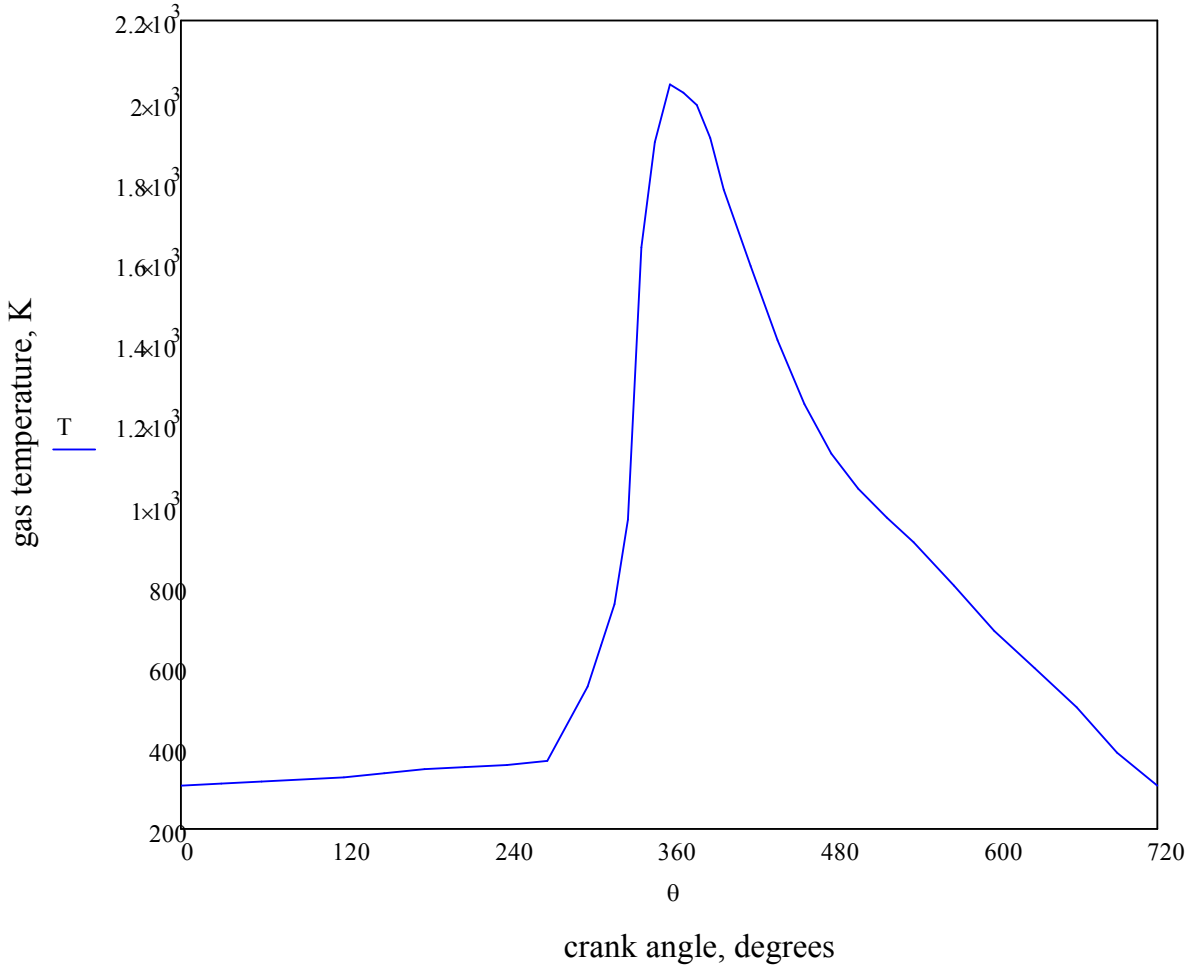

Figure 27. The gas temperature variation with crank angle.

Finally, figure 28 shows variation of heat flux over the engine cycle with crank angle. It can be seen that during the intake stroke the heat flux is slightly increasing. Air compression stroke features more rapid growth of heat flux with significant jump high to its peak value when approaching the TDC, so that the most heat energy is generated and transferred to the cylinder walls, head and piston surface near TDC. During the expansion and exhaust strokes, heat flux is on a moderate decrease.

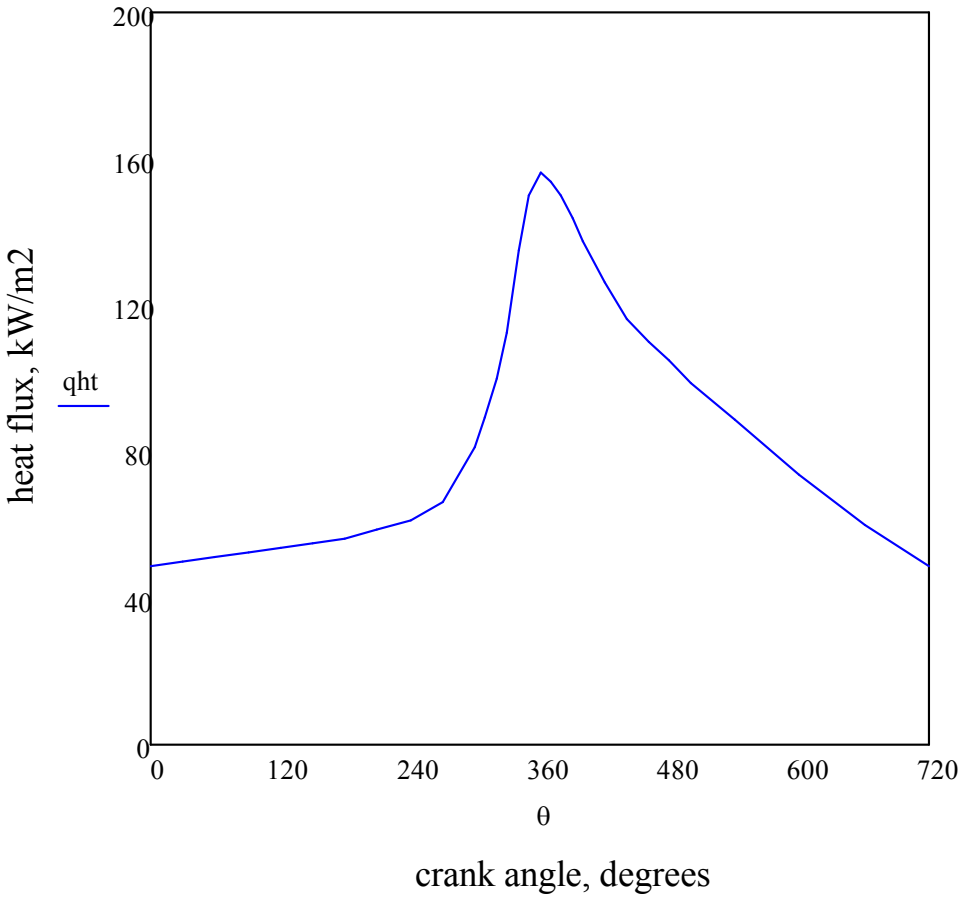

Figure 28. Heat flux variation with crank angle.

To evaluate correlations between the measured and predicted values of heat flux, the coefficient of determination R_d is used:

$$R_d = \frac{\sum_{i=1}^{n}(\hat{y}_i - \bar{y})^2}{\sum_{i=1}^{n}(y_i - \bar{y})^2}, \tag{6.2}$$

where y is the experimental data; $\bar{y}$ is the mean value of experimental data; and $\hat{y}$ is the predicted data. Typically, R_d ranges between 0 and 1. The closer is R_d to 1, the better predicted curve matches experimental results, and vice versa.

According to the heat flux values obtained thanks to simulation model, comparison with the experiment gives:

$R_d = 0.7385$.

Although, according to the previous researches, the heat transfer varies significantly (Rakopolous C. D. et al. 1999) depending on the location of measuring devices, but it is safe to say that they do follow the equivalent trend with crank angle. Interestingly, all conducted studies concerning heat transfer in the combustion chamber, as well as this investigation, state that heat flux reaches its peak value once near TDC. However, certain aspects of fuel mixing in swirl – chamber compression ignited engine, like the one under testing, feature one extra small after – peak at 70 – 80 degrees of crank angle after TDC.

7. CONCLUSION

The use of gradient heat flux sensors allow us to have the opportunities and improves possibilities to gather measurement data from different thermal experiments. In particular, it is possible to:

- use gradient heat flux sensors in the research of heat exchange under different modes of heat transfer: free and forced convection, radiation and complicated heat exchange;
- study heat exchange in devices where the unsteady character of process is essential such as combustion chamber if the internal combustion engine.

There are different important advantages of use of gradient heat flux sensor. Data, obtained with gradient sensors, allows not only to create perfect heat exchangers, but to increase thermal efficiency of different working exchangers.

There are a lot of applications of the gradient heat flux sensors. In particular, it is possible to use them in: food and chemical processing, insulation evaluation, walls, windows, roofs, flames, mass flow, endothermic and exothermic processes, medical instrumentation, hot and cold pipes, thermal property measurement, building and insulating material properties, building heating and cooling, earth, soil, agriculture, drying, curing, radiator testing, heat transfer in boundary layers. (Mityakov A. V. 2011) In my thesis I considered the use of gradient sensor in combustion chamber of the internal combustion engine. The experiment was conducted by Mityakov A. V., where gradient heat flux sensor was placed in four stroke diesel engine Indenor XL4D to measure heat flux in the combustion chamber. The results which were obtained from the experiment were compared with model's numerical output.

A one – dimensional single zone numerical model, developed by Kyung Tae Yun et al., was utilized to compare numerical results, obtained with aid of this simulation model, and data which we get from experiment. The model is acceptable due to the temperature gradient normal to the surface being larger comparing to the gradient along the surface. Different input data as bore, stroke, compression ratio, velocity etc. were used in the simulation model. Need to say that model's numerical output is quite similar with experimental results. But as we could see from the graphs, there was a certain deviation in heat flux behavior after TDC for the particular engine.

There are some explanations of difference in values between numerical and experimental results:

- this model doesn't consider the impact of fuel mixing type on combustion process and following heat flux, that's why we get such picture of the process;
- assuming the working medium as ideal gas;
- neglecting of dissociation of combustion products;
- different empiric coefficients.

We can't apply a one – dimensional single zone numerical model for motoring condition, that's why we used it only for firing conditions.

8. REFERENCES

Balagurov B.Ya. 1986. Fizika Tverdogo Tela, vol. 28.

Chang J., Fillipi Z., Assanis D., Kuo T.-W., Najt P., Rask R. 2005. Characterizing the thermal sensitivity of gasoline homogeneous charge compression ignition engine measurements of instantaneous wall temperature and heat flux. Int.J.Engine.Res. Vol.6. p. 289–309.

Cook W. J. and Felderman E. M. 1966. Reduction of data from thin film heat-transfer gages: a concise numerical technique, AIAA J., 4, 561-562.

Diller T. E. 1993. Advances in heat flux measurement, in J. P. Hartnett et al. (eds.), Advances in Heat Transfer, Vol. 23, Boston: Academic Press, 279-368.

Diller T. E. and Kidd C. T. 1997. Evaluation of Numerical Methods for Determining Heat Flux With a Null Point Calorimeter, in Proc. 43rd Int. Instrum. Symp., Research Triangle Park, NC: ISA, 357- 369.

Diller T. E. 1999. Heat Flux. Available at: http://dsp-book.narod.ru/MISH/CH34.PDF.

Divin N. P. 1998. “Heat Flux Sensor,” RF Certificate on Useful Model, No. 9959, Russian Agency on Patents and Trade Marks, August 10.

Djachenko N. H. 1974. Teorija dvigatelej vnutrennego sgoranija. Lenengrad: Mashinostroenije.

Gardon R., 1953. An instrument for the direct measurement of intense thermal radiation, Rev. Sci. Instrum., 24, 366-370.

George W. K., Rae W. J., Seymour P. J., Sonnenmeier J. R. 1991. An evaluation of analog and numerical techniques for unsteady heat transfer measurement with thin film gages in transient facilities, Exp. Thermal. Fluid Sci., 4, 333-342.

Giilhan A. 2007. Heat Flux Measurements in High Enthalpy Flows. Available at http://ftp.rta.nato.int/public//PubFulltext/RTO/EN/RTO-EN-008///EN-008-09A.pdf.

Hauser R. L. 1985. Construction and performance of in situ heat flux transducers, in E. Bales et al. (eds.), Building Applications of Heat Flux Transducers, ASTM STP 885, 172-183.

Hauser R. L. 1985. Construction and performance of in situ heat flux transducers. Building Applications of Heat Flux Transducers, pp. 172 – 183.

Heywood J. B. 1998. Internal combustion engine fundamentals. New York (USA): McGraw-Hill.

Kavtaradze R. Z. 2001. Localnyj teploobmen v porshnevyh dvigatelyah. Moscow: BMSTU.

Kidd C. T. and Nelson C. G. 1995. How the Schmidt-Boelter gage really works, Proc. 41st Int. Instrum. Symp., Research Triangle Park, NC: ISA, 347-368.

Knauss H., Gaisbauer U., Wagner S., Buntin D., Maslov A., Smorodsky B., Betz J.A. 2006. Novel sensor for fast heat flux measurements. AIAA 2006-3637.

Kostin A. K. 1989. Rabota diselej v uslovii ekspluatacii. Leningrad: Mashinostrojenije.

Kuo C. H. and Kulkarni A. K. 1991. Analysis of heat flux measurement by circular foil gages in a mixed convection/radiation environment, ASME J. Heat Transfer, 113, 1037-1040.

Kyung Tae Yun, Heejin Cho. 2012. Modeling of reciprocating internal combustion engines for power generation and heat recovery. Applied energy.

Mityakov A. V., Sapozhnikov S. Z., Mityakov V. Y., Snarskiic A. A., Zhenirovsky M. I., Pyrhnena J. J. 2011. Gradient heat flux sensors for high temperature environments.

Moffat R. J. 1990. Experimental heat transfer, in G. Hetsroni (ed.), Heat Transfer 1990, Vol. 1, New York: Hemisphere, 187-205.

Neumann D. 1989. Aerothermodynamic instrumentation, AGARD Report No. 761.

Orlin A. S., Vyrubov D. N., Ivin V. I. et al. 1971. Teorija rabochih processov porshnevyh I kombinirovannyh dvigatelej. Moscow: Mashinostrojenije.

Orlin A. S., Kruglov M. G. 1983. Dvigateli vnutrennego sgoranija. Teorija porshnevyh I kombinirovannyh dvigateley. Moscow: Mashinostrojenije.

Ortolano D. J. and Hines F. F. 1983. A simplified approach to heat flow measurement. Advances in Instrumentation, Vol. 38, Part II, Research Triangle Park: ISA, 1449-1456.

Pullins C. A., Diller T. E. 2010 In situ high temperature heat flux sensor calibration, Int. J. Heat Mass Transfer, p. 3429–3438.

Rakopolous C. D., Mavropoulos G.C. 1999. Experimental instantaneous heat fluxes in the cylinder head and exhaust manifold of an air – cooled diesel engine. Energy Conversion and Management.

Samsonov V. I. 1990. Dvigateli vnutrennego sgoranija morskih sudov. Moscow: Transport.

Sapozhnikov S. Z., Mityakov V. Yu., Mityakov A. V. 2003. Gradient Heat Flux Sensors, Saint-Petersburg State Polytechnical University, Saint-Petersburg.

Sapozhnikov S. Z., Mityakov V. Yu., Mityakov A. V. 2006. Gradient Heat-Flux Sensors: Possibilities and Prospects of Use. *Thermal Engineering*. Vol. 53, No. 4, pp. 270–278.

Sapozhnikov S. Z., Mityakov V. Yu., Mityakov A. V. 2007. Gradient Heat Flux Sensors in Heat Engineering Experiments, Polytechnical University Publisher, Saint- Petersburg.

Schultz D. L. and Jones T. V. 1973. Heat transfer measurements in short duration hypersonic facilities, AGARDograph 165.

Simeonides G., Vermeulen J. P., Boerrigter H. L. 1993. Quantitative heat transfer measurements in hypersonic wind tunnels by means of infrared thermography, IEEE Trans. Aerosp. Electron. Syst., 29, 878-893.

Snarskii A.A., Pal'ti A.M., Asheulov A.A. 1997. Fizika I Tekhnika Poluprovodnikov. vol. 31.

Sujay R.-M. 2005. Thesis for the degree of Master of Science in Mehanical Engineering, Virginia Polytechnic Institute and State University.

Terrell J. P. 1996. New high sensitivity, low thermal resistance surface mounted heat flux transducer, Proc. 42nd Int. Instrum. Symp., Research Triangle Park, NC: ISA, 235-249.

Van der Graaf F. 1989. Heat flux sensors, in W. Gopel et al. (eds.), Sensors, Vol. 4, New York: VCH, 295-322.

Vasiljev L. A. 1987. Teorija rabochih processov dvigatelej vnutrennego sgoranija: programma, metodicheskije ukazanija I kontrolnyje zadanija dlya studentov zaochnogo faculteta. Habarovsk: HPI.

Walker D. G. and Scott E. P. 1995. One-dimensional heat flux history estimation from discrete temperature measurements, in R. J. Cochran et al. (eds.), Proc. ASME Heat Transfer Division, Vol. 317-1, New York: ASME, 175-181.

Wimmer A., Pivec R., Sams T. 2000. Heat Transfer to the Combustion Chamber and Port Walls of IC Engines – Measurements and Prediction. SAE paper 2000-01-0568.

Yuh – Yih Wu, Bo – Chiuan Chen, Feng – Chi Hsieh. 2006. Heat transfer for small – scale air – cooled spark – ignition four – stroke engines. Heat and Mass Transfer.

Yusaf T. F.,Yusoff M. Z. 2005. Modeling of transient heat flux in spark ignition engine during combustion and comparisons with experiment. American Journal of Applied Sciences, vol. 2, p. 1438 – 1444.